Effect of Heat Treatment on Mechanical Properties and Microstructure of Four Different Heats of ASTM A710 Steel

G.E. Hicho, C.H. Brady, L.C. Smith, and R.J. Fields

U.S. DEPARTMENT OF COMMERCE
National Bureau of Standards
Fracture and Deformation Division
Gaithersburg, Maryland 20899

March 1985

EFFECT OF HEAT TREATMENT ON MECHANICAL PROPERTIES AND MICROSTRUCTURE OF FOUR DIFFERENT HEATS OF ASTM A710 STEEL

G.E. Hicho, C.H. Brady, L.C. Smith, and R.J. Fields

U.S. DEPARTMENT OF COMMERCE
National Bureau of Standards
Fracture and Deformation Division
Gaithersburg, Maryland 20899

March 1985

ADMINISTRATIVE INFORMATION

Effect of Heat Treatment

on

Mechanical Properties and Microstructure

of

Four Different Heats of ASTM A710 Steel

Abstract

ASTM A710 is an HSLA steel whose strength is a result of both a fine grained microstructure and a dispersion of copper precipitates. For these reasons, the tensile and impact properties of an A710 plate depend both on the thermo-mechanical history of each plate and on its chemistry. Since plates shipped from steel suppliers are frequently heat treated under different conditions, it is difficult to know whether property differences are due to chemistry variations or to heat treatment variations or vice versa. Heat to heat property differences should be determined for a specific, known heat treatment. This report describes the variability in the mechanical properties of four plates made from four different heats of steel, that have received known, and carefully controlled, heat treatments at the National Bureau of Standards. The sensitivity of these properties to heat treatment variations within each heat is also reported here. Optical and electron metallographic techniques were used to determine as-received and heat treated microstructures. Scanning electron fractography was used to ascertain the fracture mechanism in the tensile and impact tests. This report also contains two appendices in which splitting fracture and microchemistry observations in A710 are discussed.

Introduction

ASTM A710 [1]* is a fine grained, age-hardening high strength, low alloy (HSLA) steel, which derives much of its strength from fine grained ferrite containing a dispersion of ultra fine niobium carbo nitride and 10-20 nanometer diameter copper precipitates. In a previous report [2], the as-quenched yield strength (i.e. that due to the fine grained microstructure) was found to be about 414 MPa (60 ksi). In practice, the yield strength of

_____

* Refers to references located at end of report.

A710 is increased to the 552-621 MPa (80-90 ksi) range by precipitating the copper as small, dislocation impeding particles. It was shown in the report [2] that this additional strengthening can be achieved without detriment to the impact properties provided that this alloy is heat treated past the peak aged condition. In its commercially recommended heat treated form, A710 is well past the peak aged condition. One accomplishment of the previous work [2] was to determine the sensitivity of A710 to variations from recommended heat treatment, which might occur in practice. That work was carried out on one plate, and thus, represented only one heat of A710. In this task, by carefully heat treating the plates representing the four heats into the same Class 3 condition, the heat-to-heat variation in properties and microstructures were determined. Furthermore, by varying the treatments in a controlled manner, the heat-to-heat sensitivity to heat treatment was also quantified.

Earlier work [2] on this alloy had shown a tendency for some tensile specimens to split longitudinally prior to final fracture. This splitting, which appears to be an extreme form of "star" fracture, was only observed for some heat treated conditions. It was again similarly observed in the present research. Notched tensile tests, reported in Appendix A, show that the splitting requires large amounts of plastic strain and is not simply a stress state effect. While the cause of the splitting and the reason it depends on heat treatment is still unknown, the results presented here suggest that this phenomenon does not detract from the high ductility and fracture resistance of A710.

Also presented in Appendix B is a short discussion of the chemistry of micro-constituents that were found during the electron microscopic studies carried out as an extension of this work. These observations indicate that certain alloying elements may not have had sufficient time to mix completely during steel making. The occurence of an unusually high concentration of silicate inclusions in one plate which resulted in erratic impact toughness behavior is discussed.

Characterization of As-Received Plates

Four plates of A710 were supplied to the National Bureau of Standards (NBS) by David Taylor Naval Ship Research and Development Center (DTNSRDC). The plates were each approximately 0.36 m^2 (2 ft^2) by 19 mm (3/4 inch) thick. These plates were identified by DTNSRDC according to the following code.

Plate Number	Identification Code	Further details
Plate 1	GAG	Supplied as Class 3 plate to DTNSRDC Marked: HT 48259
Plate 2	FZF	Supplied as Class 1 plate to DTNSRDC Marked: P43133 HT54614
Plate 3	FZN	Supplied as rolled (for Class 3 heat treatment) Marked: HT 42781
Plate 4	FZY	Supplied as Class 1 plate to DTNSRDC Marked: HT 42781

The available mill report chemistries and check chemistries performed by DTNSRDC and NBS are reported in Table 1.

Metallographic specimens were cut about 10 cm from the edge of each plate and prepared according to the techniques described in the first report (2). Microscopic examination of the polished specimens verified that the rolling direction was as marked by DTNSRDC. The etched microstructures of the four plates are shown in Figures 1 a to d. An effective grain boundary etchant was found to be ammonium molybdenate, $(NH_4)_2 MoO_4$, and HNO_3 in ethanol. The exact preparation of this etchant is as follows:

3

<u>Stock solution-</u>

    100 ml distilled H_2O

mix

    15 grams $(NH_4)_2M_0O_4$

Then add - 100 ml HNO_3

Let stand 4 days, filter, and bottle.

<u>Etchant-</u>

Mix 2 ml of above stock solution with 100 ml ethanol. Will color ferrite after 30-45 seconds immersion.

Micrographs of GAG (fig. 1a), FZF (Fig 1b), and FZN (Fig. 1c) reveal predominantly fine grained, equiaxed ferrite typical of a Class 3 plate (3), i.e. solution quenched and aged. Note that FZF was supposed to be a Class 1 plate, i.e. as-rolled and aged. FZY (Fig. 1d) exhibits a coarser (though somewhat mixed) ferrite grain size with grains elongated by rolling. This microstructure is typical of a Class 1 plate (3) and is consistent with the reported class of this plate.

Plate FZN and to a lesser extent, plate GAG contain some non-equiaxed ferrite. The grain boundaries in these plates and in FZF are highly irregular compared to the boundaries in FZY. This roughening of grain boundaries is due to the rapid quench required for Class 3 (4). The resulting ferrite can be polygonal and acicular in habit, but its boundaries will be highly irregular or rough as observed. The rate of cooling, the austenite grain size, and the plate chemistry probably determine the amount of acicular ferrite that forms in these largely polygonal ferrite microstructures (5).

All of the plates have a small amount of a darker phase which is a carbide colony-probably a tempered martensite. The sulphide inclusions in FZF (Fig. 1b) are completely spheroidized indicating that this steel has been desulphurized and either calcium or rare earth treated. Some of the inclusions in FZN (fig. 1c) appear to be somewhat rounded as though a partial treatment had taken place. FZY (Fig. 1d) and GAG (Fig. 1a) have long sulphide stringers and there is no evidence that these heats, represented by the two plates, received any inclusion spheroidizing treatment. The grain sizes of the as-received plates are given in Table 2. The grain sizes were determined by

the planimetric (or Jeffries) procedure (6). Due to the irregularity of some grain boundaries, the grain size may have an error of ± 1/2 ASTM grain size number. The larger, mixed grain size of FZY is consistent with it being in the Class 1 condition. Again, the small grain size of FZF is not consistent with its reported class. The microstructure studies so far suggest that FZF was, in fact, in the Class 3 condition.

Transmission electron microscopy[*] of GAG, FZF, and FZY (Fig. 2a) revealed the presence of the small copper precipitates responsible for the age hardening behavior of this alloy. However, these precipitates are not visible in a similar electron micrograph of FZN (Fig. 2b). Note that there are several bend contours and orientations in Fig. 2b so that particle invisibility is not due to missing the diffraction condition. At very high magnifications, and in a high resolution STEM, 10 nm precipitates are faintly visible in FZN (Fig. 3). As discussed in the previous report (2) and elsewhere (7), copper precipitates in BCC iron have practically no electron contrast mechanism while they are coherent. Once coherency is lost, the copper takes up its FCC form and the structure factor difference will provide ample contrast. Loss of coherency occurs near the peak aged condition (7) and fairly large (5-10 nm) copper precipitates should begin appearing. This is just what was observed for FZN suggesting that FZN was near the peak aged condition or slightly underaged.

For verification, small coupons of FZN were heated at 482°C (900°F) for varying times. If underaged, A710 will harden slowly at 482°C (900°F). Indeed, the data (Fig. 4) seem to show a slight hardening with time. This verified that the as-received FZN plate was indeed underaged or near the peak aged condition. As will be discussed later, reheat treatment of this plate uncovered additional anomalous behaviors.

---

[*]Foils were prepared by jet electropolishing in a chilled ethanol-perchloric acid solution.

5

Table 3 shows the mechanical properties, supplied by DTSNRDC, for the as-received 19 mm (3/4 inch) thick A710 plates studied, and the ASTM specifications for each particular class.

All of the plates, GAG, FZF, FZY, and FZN met the tensile requirements for their respective classes and thickness. Plates GAG, FZF, and FZN met the impact requirements, but plate FZY was found to be deficient. The proposed reasons for its impact energy being lower than 20 J (15 ft-lbs) at -46°C (-50°F) will be presented later.

Heat Treatment Procedures

Three test coupons were cut from each as-received plate. These test coupons were approximately 152 mm (6 inches) long, 63.5 mm (2.5 inches) wide and 19 mm (3/4 inch) thick. All the coupons were austenitized at 899°C (1650°F) for 68 minutes followed by a quench into a water bath maintained at 21°C (70°F). The choice of aging temperatures were 538°C (1000°F), 593°C (1100F), and 649°C (1200°F). Coupons were aged at this temperature for 30 minutes. A total of 3 heat treatment variations were performed on each plate. The times to attain the austenitizing and aging temperatures were determined prior to heat treating. These times were added to the austenitizing and aging times so that times quoted above represent time-at-temperature.

Preparation of Test Specimens

The specimens used for the tensile tests were 12.7 mm (.500 inch) in diameter and dimensioned according to ASTM Specification A370, Part 10, 1982 (8). The Charpy V-notch specimens were prepared and tested according to ASTM Specification E23-82 (9). The notches were placed in the specimen with a broaching tool for reproduceability. The specimens were taken as close as possible to the quarter-thickness location in the plate. The tensile specimens were oriented with their longitudinal axes transverse to the rolling direction. The orientation of the CVN specimens corresponded to the ASTM TL direction (9); that is, the axis was transverse to the rolling direction of the plate and the notch located parallel to the rolling direction. It should be noted that each individual heat treatment was performed on each coupon prior to machining. Two tensile and Charpy tests were performed for each heat treatment variation.

Test Conditions

The tensile specimens were tested at room temperature using a universal testing machine. Calibration data for the testing machine indicated that the accuracy of the load readings was within ±1/2% as specified by ASTM E-4 (10). An extensometer was placed on the specimen to measure the percent strain over a 50 mm (2 inch) gage length. ASTM specification A370, part 10, 1982 (8) recommended the loading rate be 0.01 in/in/min prior to yield, then 0.1 in/in/min after yield for a specimen having a gage length of 50 mm (2 inches).

The CVN specimens were tested at -17.8°C (0°F) according to ASTM specification E23-82 (9). They were immersed in the bath medium (ethyl alcohol) and held at temperature for at least 30 minutes before testing. The bath was magnetically stirred and the temperature was constantly monitored with a thermocouple.

Tensile Test Results

Table 4 shows the tensile test results. Figures 5, 6, and 7 indicate how the 0.2% yield strength, ultimate tensile strength, reduction-in-area, and elongation-to-fracture vary with precipitation hardening temperature and time. Most tensile stress-strain curves exhibited a yield drop. The 0.2% offset yield strength is approximately equal to the lower yield strength. The UTS and yield strength both decrease with increasing aging temperature. This indicates that these heat treatments are all past the peak aged condition of this alloy.

Figure 7 shows the reduction-in-area and elongation-to-fracture in 50 mm (2 inches) for the test plates as a function of precipitation hardening temperature and time. The elongation is essentially uniform throughout the hardening range, and there appears to be no significant difference between the elongation values for each of the plates. The reduction-in-area values are somewhat different. The most noticeable difference occurs in plate FZN. Plate FZN has the lowest reduction-in-area as a function of precipitation hardening temperature and grain size. Longitudinal splitting of the tensile specimens was observed for a few specimens. This phenomenon does not detract

7

from the uniaxial ductility and, as discussed in Appendix A, apparently does not indicate any potential ductility problem with A710. In three of the tensile tests, the upper yield strength was slightly greater than the UTS. This only occurred in plate GAG when the test coupon was precipitation hardened at 649°C (1200°F). In plate FZF, two test coupons, both precipitation hardened at 649°C (1200°F) also showed the same phenomena - the upper yield strength was greater than the UTS. This might cause concern in load controlled situations and compliant structures. Figure 8 was developed to show the relationship that exists between the upper yield and lower yield strengths for the four plates as a function of aging conditions. Large yield drops are observed in plates GAG, FZF, and FZY; yield drops are small or absent in plate FZN.

Impact Test Results

The -17.8°C (0°F) impact test results are listed in Table 3 and plotted in Figure 9 as a function of aging time and temperature. For all plates, the toughness increases with increasing time and temperature. As shown in the last section, this alloy is overaged in all the heat treated conditions investigated here and the increasing toughness with aging is consistent with that. As with tensile ductility, we note that plate FZN was the least tough for all aging conditions examined. Indeed, this plate exhibited the lowest CNV energy, i.e. 67.8 J (50 ft-lbs), of any Class 3 heat treated A710 material ever examined at NBS. Figure 10 is a plot of the lateral expansion as a function of precipitation hardening temperature. Plate FZN shows the least lateral expansion at each of the aging conditions. Plate FZF shows the most consistent lateral expansion over the hardening range.

Figure 11 is a plot of UTS and yield strength versus toughness. This graph demonstrates the typical trade off between toughness and strength for different aging treatments. However, some plates (i.e. different heats) offer much better combinations of strength and toughness than other plates. From this figure we note that FZN offers the least desirable combination of properties. For any given strength level, FZN has significantly less impact fracture resistance than any of the other plates. The general inverse correlation between strength and toughness does not hold when comparing different heats of A710. This point will covered more fully in the Discus-

8

sion section.

Hardness Test Results

The hardness test results using a Knoop indenter are shown in Table 5. Knoop hardness was used because these units are more linear over the desired hardness range than Rockwell hardness. The Knoop units can be related to the Rockwell A, B, and C values shown in the table. The results appear to be consistent with those obtained in the previous report (2).

Microstructure of Heat Treated Plate

The specimens used for microstructural analysis were taken from broken impact specimens. Specimens representative of each plate and each precipitation hardening treatment were mounted, polished, etched, and examined. These metallographic specimens indicated that the microstructure observed in the optical microscope was not altered from the as-quenched microstructure by any of the aging treatments. This is in accord with previous work (2). We therefore include here micrographs of only the 30 minutes at 593°C (1100°F) aging treatment for each plate. These are typical of the optically resolvable microstructure for the other aging treatments as well. Figures 12 and 13 are photomicrographs of the heat treated plates at X500 and X1250 magnifications, respectively. It should be noted that all of these specimens represent material heat treated to the Class 3 condition. Plates GAG, FZF and FZY, at X500, reveal very fine ferrite microstructures. It is plate FZN's microstructure that appears to be a little coarser. The grain size of these heat treated plates are listed in Table 2. At X1250 magnification, the microstructures of plates GAG and FZY, Figures 13a and 13d, are primarily a fine polygonal ferrite with some small amount of carbide phase and acicular ferrite. Overall, plates GAG, FZY, and FZF appear similar, but FZF has a finer ferrite grain size.

Figure 13c, a micrograph of plate FZN at X1250, shows a microstructure unlike the other three plates. The ferrite has more acicular grains present and both the polygonal and equiaxed grains are relatively large. Larger colonies of a carbon-rich phase are visible in this plate (Fig. 12c) compared to the others. Although NBS definitely heat treated this plate to a Class 3 condition, FZN does not exhibit a microstructure typical of A710 in any of

9

the three classes (3).

Table 6 shows a summary of properties for the as-received plates, and the same plates heat treated to the class 3 condition. Most noticeable is the increase in the impact properties obtained after heat treating for plates FZN and, in particular, FZY. Plate FZY's impact property increased dramatically, from 11 J (8ft-lbs) to 161 J (119 ft-lbs) when tested at -17.8°C (0°F).

Discussion

In the studies described above, numerous references have been made to the anomalous behavior of metal from the FZN plate. Prior to the onset of the work at NBS, researchers at DTNSRDC had observed unusually poor impact resistance in specimens taken from this plate (see Table 3). It is instructive to hypothesize as to why FZN behaves as it does, for this will lead to a greater understanding of A710 in general. Many of the details that assist in an understanding of FZN have already been presented in this report. As shown in Table 1, the chemistry for this plate is not typical of A710 since the Al content is low. The optically resolvable microstructure of the as-received FZN plate looks fairly typical of A710 Class 3. The electron metallography indicates that the copper precipitates are just losing coherency with the matrix. This suggests that the as-received FZN plate is in the peak aged condition which is less tough than the overaged condition. The peak aged condition was further verified by continued aging at 482°C (900°F). And finally, reheat treatments, which should have brought FZN into a Class 3 condition, resulted in a microstructure and properties that are not typical of A710 in the Class 3 condition. The grains had pronounced acicular habits and were larger than the grains in the other plates. DTNSRDC researchers have also associated this type of microstructure with reduced impact properties.

The reason for the low impact properties obtained on plate FZN could possibly be attributed to the grain size of the steel. Normally the steel should have a fine acicular ferrite/polygonal ferrite microstructure (5). This final microstructure is the result of niobium and aluminum's ability to promote a fine grain size. The fine ferrite structure leads to improved mechanical properties. For good grain size control, aluminum levels should

10

be about 0.025 to 0.030 weight percent. Aluminum was found to be 0.016 weight percent. With reduced Al content, austenite grain coarsening could occur which would lead to a larger ferrite grain size than desired[*]. This coarse grain size would then lead to lower impact properties. Due to the low Al content FZN is not typical of A710. Therefore, the conclusions concerning the sensitivity of A710 to heat treatment variation will be made excluding the data obtained on FZN.

Examining first the yield strength (Figure 5) as a function of aging, we note that the data extends from a low of about 552 MPa (80 ksi) for GAG aged at 649°C (1200°F) to a high of about 696 MPa (101 ksi) for FZF aged at 538°C (1000°F). The average value of yield strength for the manufacturer's recommended aging treatment is 634 MPa (92 ksi). The recommended heat treatment is 899°C (1650°F), 69 min, WQ - 593 °C (1100°F), 30 min, AC. In this condition GAG yields at 600 MPa (87 ksi), FZY at 627 MPa (91 ksi), and FZF at 662 MPa (96 ksi). From these three heats of A710, it may be concluded that the yield strength (0.2% offset) will be 634 MPa ± 34 MPa (92 ksi ± 5 ksi) when heat treated according to the recommended schedule. If the aging temperature differs by 55°C (100°F) from the 593 °C (1100°F) recommended value, then the range will be larger: 620 MPa ± 69 MPa (90 ksi ± 10 ksi). For any given aging treatment, FZF is always stronger than FZY, which is always stronger than GAG. This difference can be attributed to grain size differences among the plates (Table 3). The smaller the grain diameter, the stronger the alloy - as predicted by the Hall-Petch theory (11,12).

The same order of strengths holds true for the UTS (Figure 6). This behavior can again be attributed to the grain size effect. Figure 6 also shows that plates heat treated according to manufacturer's recommendation have a UTS of 703 MPa ± 27 MPa (102 ± 4 ksi). When the aging temperature is varied by 55°C (100°F), the range is increased to ± 90 MPa (±13 ksi).

---

[*] It is also possible that overheating or slack quenching after rolling coarsened the niobium carbo-nitride distribution in a way that cannot be changed by austenitizing at 899°C (1650°F). This, too, might result in coarse ferrite grains. There is, however, no evidence at present to support this possibility.

One advantage of deriving significant levels of strengthening by grain refining is that the impact properties are simultaneously improved. This is apparently also the case for A710. The strongest plate, i.e. FZF, is shown in Figure 9 to be the toughest plate as well. This is most likely due to its fine grain size. A Hall-Petch (11,12) type plot is shown in Figure 14 for strength. There appears to be some reversal of this grain size trend for GAG and FZY, but the data is so close for these two that such a conclusion is not justified. Quantitatively, the Charpy energy at -17.8°C (0°F) for these three heats is 176 J ± 25 J (130 ± 15 ft-lbs) if heat treated as recommended by the manufacturer, and 163 J ± 54 J (120 ± 40 ft-lbs) if the aging temperature is allowed to vary by 55°C (100°F).

Figure 11 plots the strength versus the toughness of all the plates. For any given plate, the higher the strength level, the lower the toughness level. This is a typical correlation for precipitation hardening alloys used past their peak-aged condition. However, the strongest plate, FZF, is also the toughest plate. This results from the small grain size. Clearly, steel chemistries and thermo-mechanical treatments which produce fine (10 micro-meter diameter) polygonal grains of ferrite will result in the best combination of strength and toughness for all common aging treatments of A710.

Conclusion

From the studies performed here on plates which are typical of A710 (i.e. FZF, FZY, and GAG), the following conclusions may be drawn:

1. With the manufacturer's recommended heat treatment, 19 mm (3/4 inch) thick, Class 3 A710 plate will have a 0.2% offset yield strength of 634 MPa ± 34 MPa (92 ± 5 ksi), a UTS of 703 MPa ± 27 MPa (102 ± 4 ksi) at 22°C, and a Charpy energy at -17°C (0°F) of 183 J ± 20 J (135 ft lbs ± 15 ft-lbs).

2. If the aging temperature varies by ± 55°C (100°F) from the recommended 593°C (1100°F), then the room temperature yield strength will be 620 MPa ± 69 MPa (90 ± 10 ksi), the UTS will be 703 MPa ± 90 MPa (102 ± 13 ksi), and the Charpy energy at -17.8°C (0°F) will be 163 J ± 54 J (120 ± 40 ft-lbs).

3. The observed plate-to-plate or heat-to-heat variation in properties can be, in part, attributed to grain size variations. In general, the room temperature yield strength, the UTS, and the Charpy energy at -17.8°C (0°F) all increase with decreasing grain size.

4. The observed variation of properties caused by heat treatments within each plate can be attributed to variations in Cu precipitate size and distribution.

5. Ductility is fairly constant for all plates and heat treatments. The elongation to fracture in a 50 mm (2") gage section is 26 ± 2% and the reduction in area is 74 ± 5% for all plates and heat treatments.

In addition to the above conclusions on typical A710 material, work on the plate FZN, which was atypical of A710, particularly in its low toughness, yielded this final conclusion:

6. The appearance of coarse grains seems to be associated with reduced impact properties and this may be the result of low aluminum content in the plate.

References

1. American Society for Testing and Materials, Annual Book of ASTM Standards, Specification A710-79, Low-Carbon Age-Hardening Nickel-Copper-Chromium-Molybdenum-Columbium and Nickel-Copper-Columbium Alloy Steels, Part 4, pp 782-785, 1982.

2. G.E. Hicho, L.C. Smith, S. Singhal, and R.J. Fields, "Effect of Thermal Processing Variations on the Mechanical Properties and Microstructure of a Precipitation Hardening HSLA Steel," Journal of Heat Treating, 3, #3, June 1984; and National Bureau of Standards Internal Report, NBSIR #83-2685.

3. R.J. Jesseman and G.J. Murphy, "High Strength Precipitation Hardened Alloy Steel for Heavy Section Applications," presented at 1977 Triple Engineering Show and Conferences, Chicago, Illinois, October 26, 1977.

4. Erkki O. Rasanen, "The Massive Transformation in Some Iron-Based Alloys," Thesis for the degree of Doctor of Technology, Technical university, Otaniemi- Helsenhi, 1969.

5. L. Meyer, F. Heisterkamp, and W. Mueschenborn, "Columbium, Titanium, and Vanadium in Normalized, Thermo-Mechanically Treated and Cold-Rolled Steels," in MicroAlloying 75, Proceedings of an International Symposium on High-Strength, Low Alloy Steels, Edited by M. Korchynsky, (1977).

6. American Society for Testing and Materials, Annual Book of ASTM Standards, Designation E112-82, Standard Methods for Determining Average Grain Size, Volume 3.03, pp 121-155, 1983.

7. E. Hornbogen, "Aging and Plastic Deformation of an Fe-0.9% Cu Alloy," Transactions ASM, Vol. 57, 1964, pp.120-132.

8. American Society for Testing and Materials, Annual Book of ASTM Standards, Designation A370-77, Standard Methods and Definitions for Mechanical Testing of Steel Products, Volume 3.01, pp 1-56, 1983.

9. American Society for Testing and Materials, Annual Book of ASTM Standards, Designation E23-82, Standard Methods for Notched Bar Impact Testing of Metallic Materials, Volume 3.01, pp 198-221, 1983.

10. American Society for Testing and Materials, Annual Book of ASTM Standards, Designation E4-83, Standard Methods for Load Verification of Testing Machines, Volume 3.01, p 101-108, 1983.

11. E.O. Hall, Proc, Phys. Soc. 64B, p 747, (1951).

12. N.J. Petch, J. Iron and Steel Inst. 173, p25, (1953).

Table 1. Mill Ladle Chemistry and Check Chemistry on Plates Studied by NBS.

Material Code	Type of Analysis	Chemical Composition (wt %)										
		C	Mn	P	S	Si	Cr	Ni	Mo	Cu	Nb	Al
GAG	Ladle	.04	.51	.010	.009	.31	.68	.93	.20	1.20	.042	-
	Check	.04	.53	.005	.005	.34	.62	.92	.15	-	-	.03
	NBS	.04	.48	<.005	.006	.30	.66	.91	.18	1.17	.033	.028
FZF	Ladle	.05	.54	.010	.006	.26	.72	.91	.20	1.20	.036	-
	Check	.06	.52	.008	.009	.27	.75	.90	.21	1.10	.047	.042
	NBS	.06	.50	.006	.007	.24	.70	.88	.18	1.19	.038	.035
FZN	Ladle	.05	.52	.010	.009	.27	.76	.90	.20	1.20	.037	-
	Check	.07	.51	.002	.003	.30	.83	.89	.22	1.26	-	.01
	NBS	.05	.51	<.005	.007	.24	.73	.89	.18	1.18	.028	.016
FZY	Ladle	.05	.52	.010	.009	.27	.76	.90	.20	1.20	.037	-
	Check	.03	.50	.004	.006	.34	.66	.93	-	1.26	-	.05
	NBS	.05	.49	<.005	.007	.30	.66	.90	.18	1.16	.027	.034
ASTM A 710 Grade A		.07 max	.40-.70	.025 max	.025 max	.35 max	.60-.90	.70-1.00	.15-.25	1.00-1.30	.02 min	* *

* not required for analysis

Table 2. Grain Sizes of As-Received and Heat Treated Plates

Plate	Condition	Average Grain Area (μm^2)	Average Grain Diameter (μm)	A.S.T.M. Grain Size Number
GAG	as-received	24.5	4.95	12-12.5
	heat treated	20.3	4.51	12.5-13
FZF	as-received	16.8	4.10	13
	heat treated	8.2	2.86	14
FZN	as-received	13.0	3.61	13-13.5
	heat treated	25.3	5.03	12-12.5
FZY	as-received	44.2	6.65	11.5
	heat treated	19.6	4.43	12.5-13

Table 3. As-Received Properties of Plates Studied by NBS (Transverse Orientation). (Plates are 3/4 inch thick)

Material code	Class	0.2% offset yield strength (MPa) (ksi)		Ultimate Tensile strength (MPa) (ksi)		Elongation in 50mm (12") (%)	Reduction in Area (%)	Charpy V-Notch Impact Energy J (ft-lb)				
								RT	-18°C 0°F	-34°C -30°F	-51°C -60°F	-84°C -120°F
GAG	3	601	87.1	700	101.5	27	70	190 (140)	145 (107)	134 (99)	113 (83)	71 (52)
FZF	1	630	91.3	719	104.3	28	75	217 (160)	226 (167)	222 (164)	184 (136)	160 (118)
FZN as-rolled		657	95.3	739	107.2	26	72	125 (92)	84 (62)	56 (41)	42 (31)	7 (5)
FZY	1	611	88.6	738	107.0	32	63	52 (38)	11 (8)	15 (11)	5 (4)	4 (3)
ASTM A 710	1	552	80	621	90	20	-		20J (15 ft-lb) @ -50°F (@ -46°C)			
Grade A (minimum)	3	517	75	586	85	20	-		68J (50 ft-lb) @ -80°F* (@ -62°C)			

* If involved as a supplementary requirement

18

Table 4. Tensile and Impact Test Results

Plate	Aging Temp. °C (°F)	Yield Stress (.2%) MPa (ksi)	Upper Yield MPa (ksi)	Lower Yield MPa (ksi)	UTS MPa (ksi)	Elongation to fracture in 2" (%)	Reduction in Area (%)	CVN Impact Energy* Joules (ft-lbs)
GAG	649(1200)	546(79.2)	612(88.2)	533(77.3)	606(88.0)	26.6	78.6	220(162)
	649(1200)	551(79.9)	613(88.9)	541(78.5)	621(90.1)	27.2	77.8	209(154)
	593(1100)	597(86.6)	656(95.2)	593(86.0)	678(98.4)	28.3	76.1	175(129)
	593(1100)	607(88.1)	663(96.2)	607(88.1)	686(99.5)	27.2	73.0	155(114)
	538(1000)	639(92.8)	680(98.7)	639(92.8)	737(106.9)	26.4	72.4	111(82)
	538(1000)	653(94.7)	684(99.3)	653(94.7)	744(108.0)	25.4	71.6	130(95)
FZF	649(1200)	626(90.8)	687(99.7)	608(88.2)	673(97.7)	25.0	78.2	216(159)
	649(1200)	604(87.7)	683(99.1)	597(86.6)	661(95.9)	27.4	78.7	237(175)
	593(1100)	673(97.6)	736(106.8)	666(96.7)	742(107.7)	28.7	75.8	202(149)
	593(1100)	655(95.0)	712(103.4)	655(95.0)	732(106.3)	25.6	76.0	201(148)
	538(1000)	697(101.2)	744(108.0)	697(101.2)	791(114.8)	27.9	71.5	159(117)
	538(1000)	707(102.6)	744(108.0)	707(102.6)	797(115.7)	25.1	71.2	190(140)
FZN	649(1200)	599(86.9)	597(86.6)	601(87.2)	655(95.1)	25.2	74.1	155(114)
	649(1200)	586(85.1)	627(91.0)	586(85.1)	656(95.2)	24.5	73.8	144(106)
	593(1100)	624(90.6)	654(94.9)	624(90.6)	692(100.5)	27.2	72.4	113(84)
	593(1100)	628(91.2)	666(96.6)	628(91.2)	701(101.7)	24.8	71.4	130(96)
	538(1000)	706(102.5)	725(105.2)	706(102.5)	781(113.4)	24.3	68.5	71(52.5)
	538(1000)	690(100.2)	717(104.0)	690(100.2)	772(112.1)	22.8	68.3	62(46)
FZY	649(1200)	587(85.2)	651(94.5)	575(83.5)	650(94.3)	26.8	76.5	178(131)
	649(1200)	573(83.2)	633(91.8)	562(81.5)	638(92.6)	25.2	75.7	161(133)
	593(1100)	635(92.2)	690(100.1)	635(92.2)	716(103.9)	25.2	73.5	161(119)
	593(1100)	629(91.3)	691(100.3)	625(90.7)	710(103.0)	25.1	73.2	161(119)
	538(1000)	692(100.4)	728(105.6)	692(100.4)	781(113.4)	25.4	69.8	107(79)
	538(1000)	701(101.8)	735(106.7)	701(101.8)	786(114.1)	26.7	70.2	104(77)

* @ -17.8°C (0°F)

19

Table 5. Hardness Test Results

Plate	Aging Temp. $^oC(^oF)$	Knoop Hardness Kg/mm^2	Rockwell A	B	C	Yield Stress MPa (ksi)	UTS MPa(ksi)
GAG	649(1200)	225	57	93	-	549(79.6)	614(89.1)
	593(1100)	256	60	98	-	602(87.4)	682(99.0)
	538(1000)	274	62	-	23	646(93.8)	741(107.5)
FZF	649(1200)	240	60	98	-	615(89.2)	667(96.8)
	593(1100)	261	61	-	20	664(96.3)	737(107.0)
	538(1000)	273	64	-	26	702(101.9)	794(115.3)
FZN	649(1200)	241	61	-	20	593(86.0)	656(95.2)
	593(1100)	251	60	98	-	626(90.9)	697(101.1)
	538(1000)	287	63	-	25	698(101.4)	777(112.8)
FZY	649(1200)	242	58	95	-	580(84.2)	644(93.5)
	593(1100)	259	60	98	-	632(91.8)	713(103.5)
	538(1000)	280	62	-	23	697(101.1)	784(113.7)

Table 6. Summary of Properties of Plates Comparing As Received to Class 3 Re-Heat Treatment.

Condition	Material Code	Class	Average Grain Size (ASTM #)	Yield Strength MPa	(ksi)	Ultimate Tensile Strength MPa	(ksi)	Elongation in 50 mm (2 inch) (%)	Reduction of Area (%)	Charpy V-Notch Impact Energy at -17.8°C (0°F) J	(ft-lb)
As-Received	GAG	3	12 - 12.5	601	(87.1)	700	(101.5)	27	70	145	(107)
	FZF	3	13	630	(91.3)	719	(104.3)	28	75	226	(167)
	FZN	as-rolled	13 - 13.5	657	(95.3)	739	(107.2)	26	72	84	(62)
	FZY	1	11.5	611	(88.6)	738	(107.0)	32	63	11	(8)
Re-Heat Treated to Class 3 1650°F-68 min Water Quench +1100°F -30 minutes Air Cool	GAG	3	12.5 - 13	602	(87.3)	683	(99.0)	28	75	164	(121)
	FZF	3	14	664	(96.3)	738	(107.0)	27	76	201	(148)
	FZN	3	12 - 12.5	627	(90.0)	697	(101.1)	26	72	122	(90)
	FZY	3	12.5 - 13	632	(91.7)	713	(103.4)	25	73	161	(119)

21
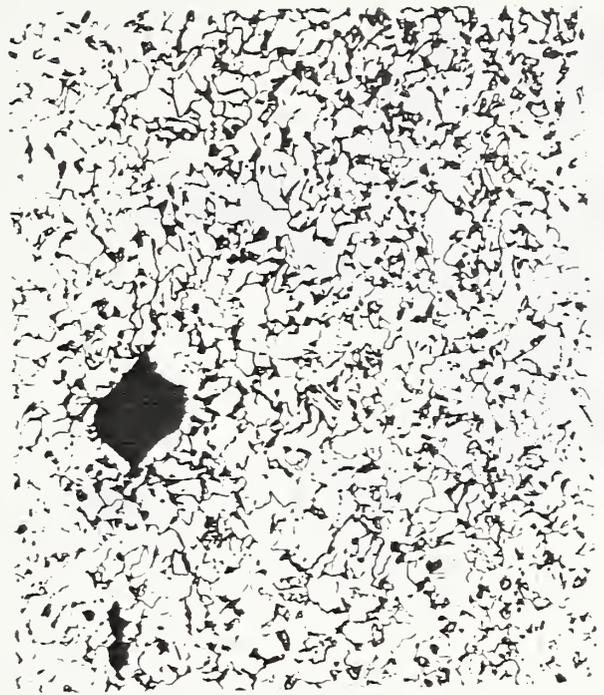
Figure 1   Etched microstructures of as-received plates;
a) GAG, b) FZF, c) FZN, and d) FZY.   All long-
tudinal sections at X500 magnification.
Etchant: $(NH_4)_2M_oO_4$ - HNO_3 solution.

22

a   b

Figure 2   Electron micrographs of (a) as-received GAG
           (typical of FZF and FZY), X60,000 and (b)
           as-received FZN, X80,000.   Precipitates clearly
           visible in GAG are not seen in FZN.

Figure 3   High resolution TEM micrograph of FZN showing faint
           contrast of precipitates, X200,000.

AGING CURVE FOR FZN AT 900 F
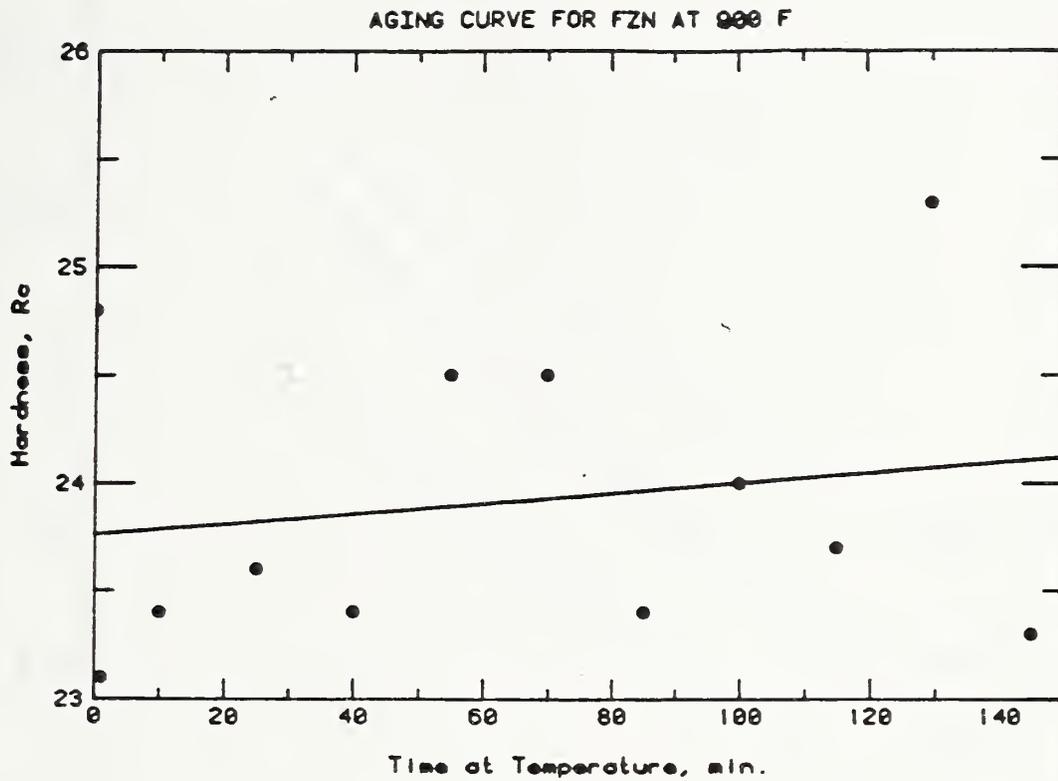
Figure 4   Effect of additional aging of FZN at 482°C (900°F)
on hardness. Observed trend indicated slight hard-
ening which can only occur in near peak hardened
material.
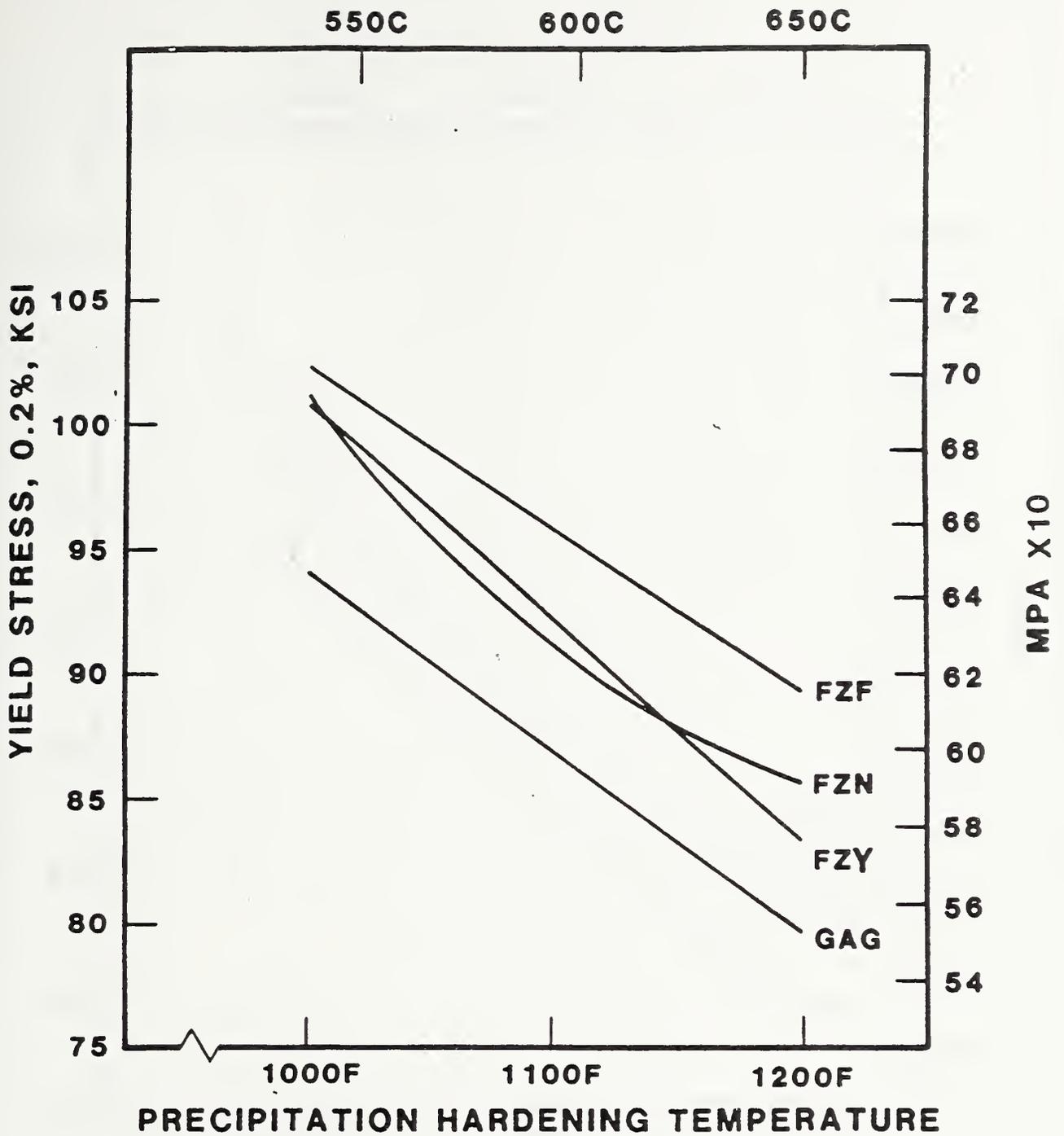
Figure 5 Yield strength as a function of aging temperature.
All samples aged for 30 minutes.
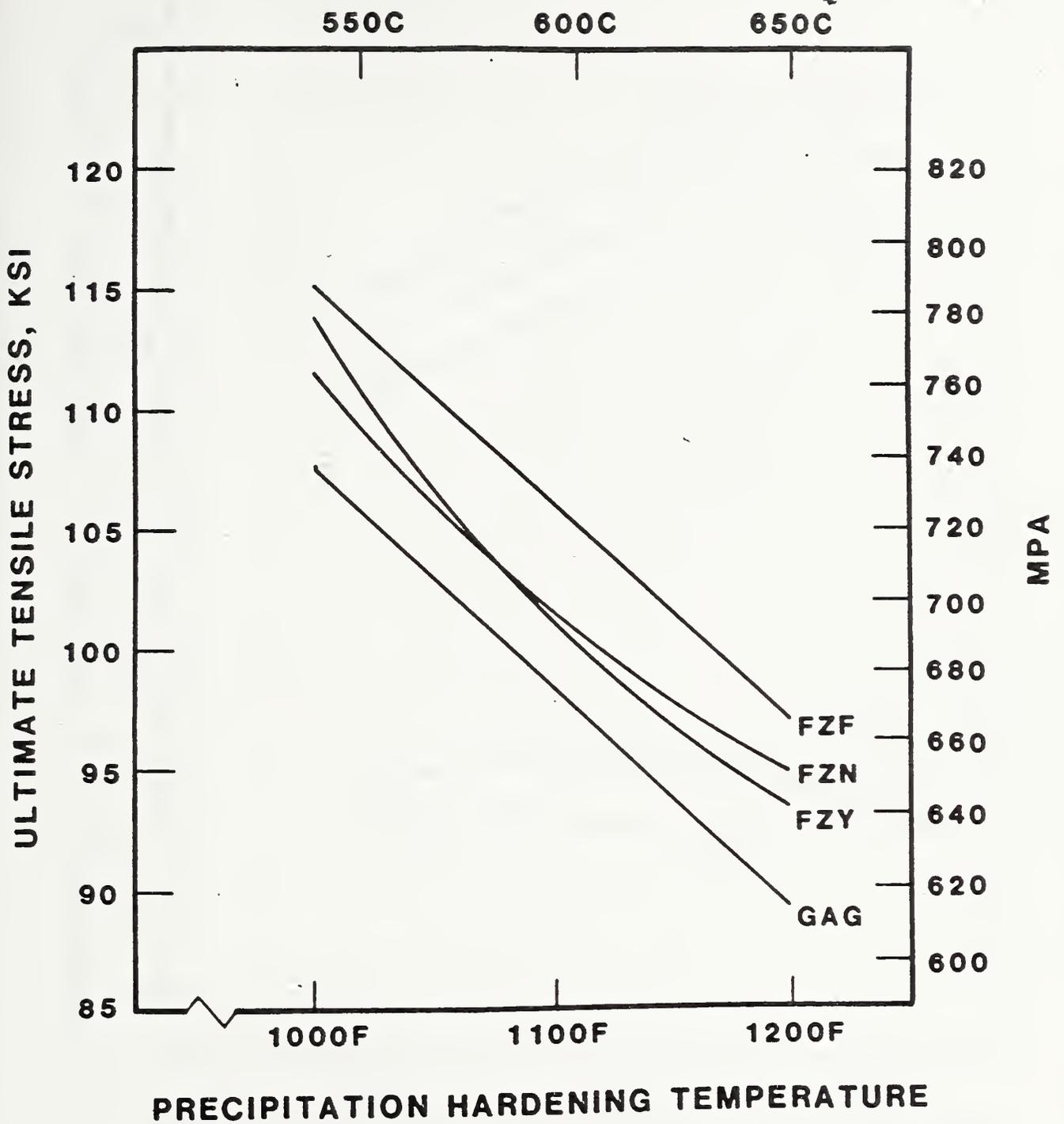
Figure 6   UTS as a function of aging temperature.   All samples
aged for 30 minutes.
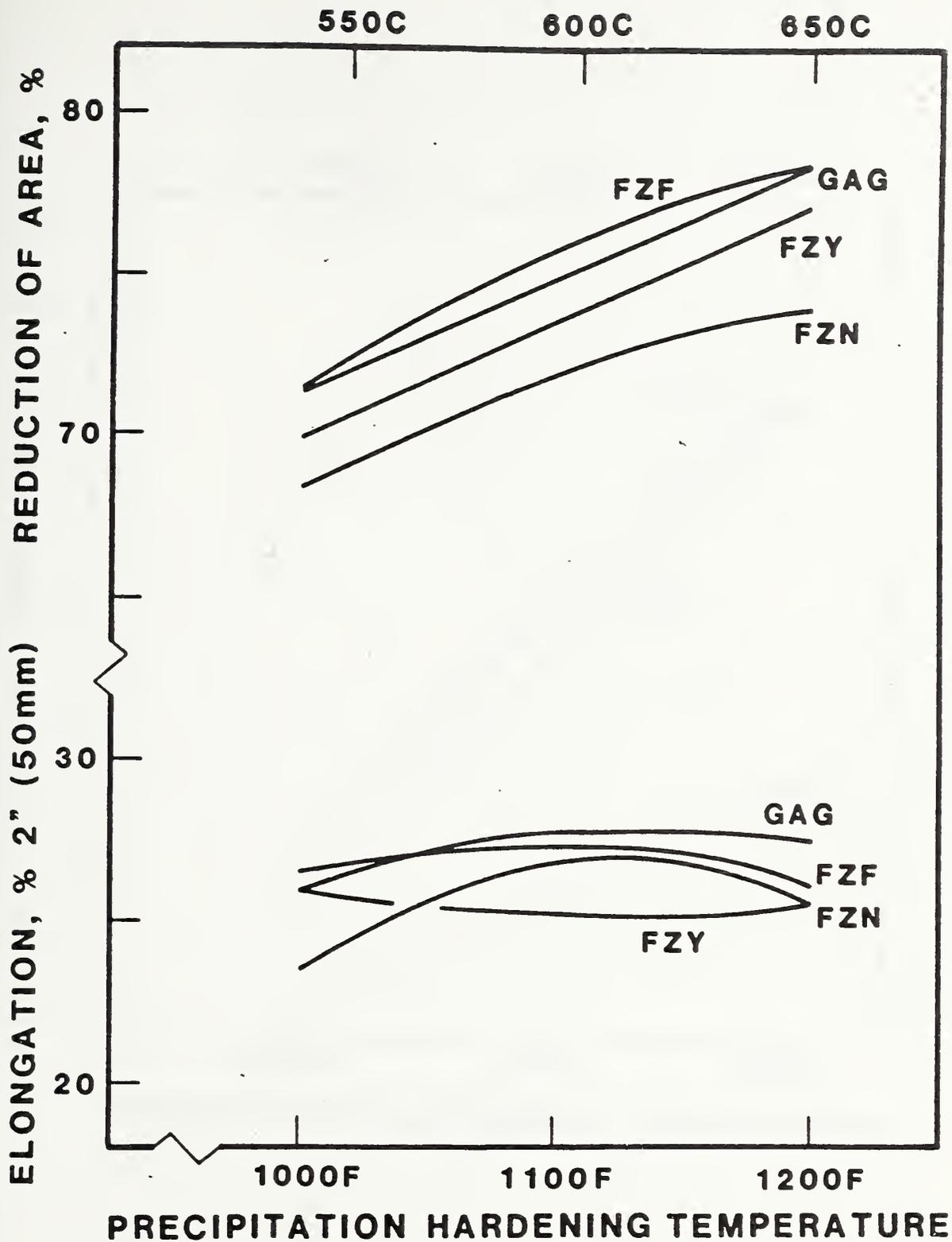
Figure 7   Reduction-in-area and elongation-to-fracture (in 2")
as a function of aging temperature.   All samples aged
for 30 minutes.
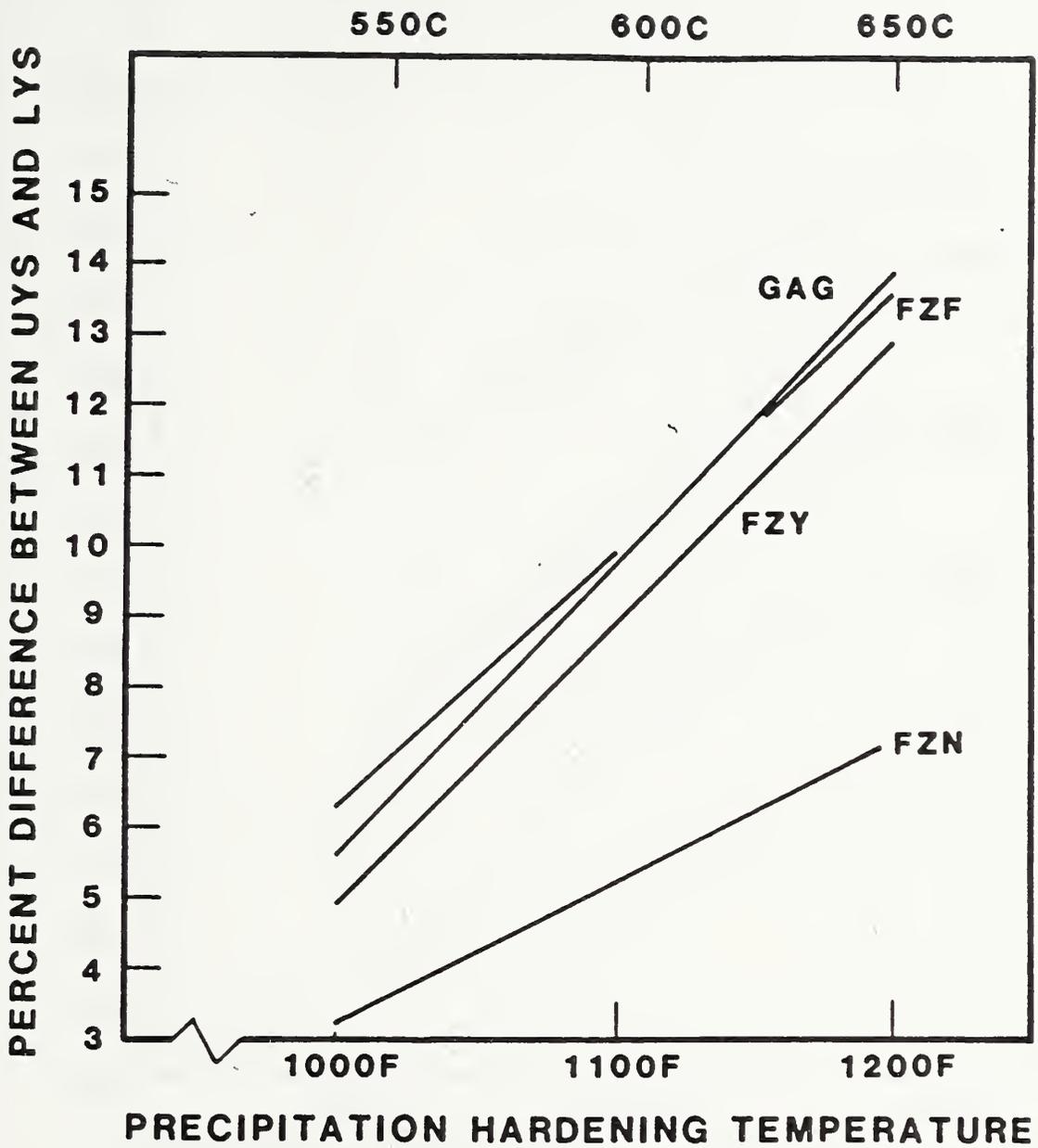
Figure 8 Percent difference between upper yield and lower
yield strength as a function aging temperature.
All samples aged for 30 minutes.
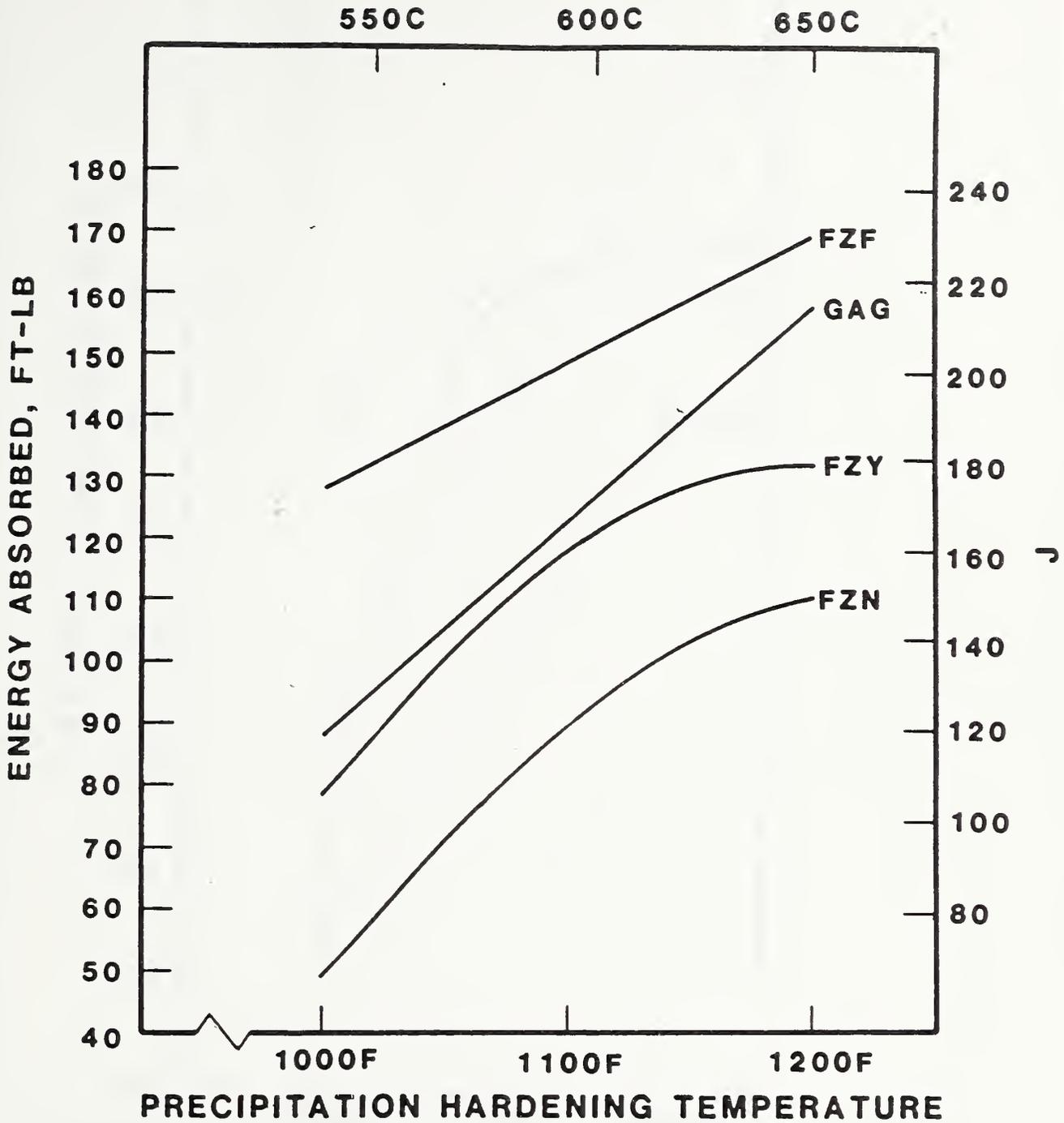
Figure 9   Energy absorbed in CVN impact tests at -17.8°C (0°F)
as a function of aging temperature. All samples aged
for 30 minutes.
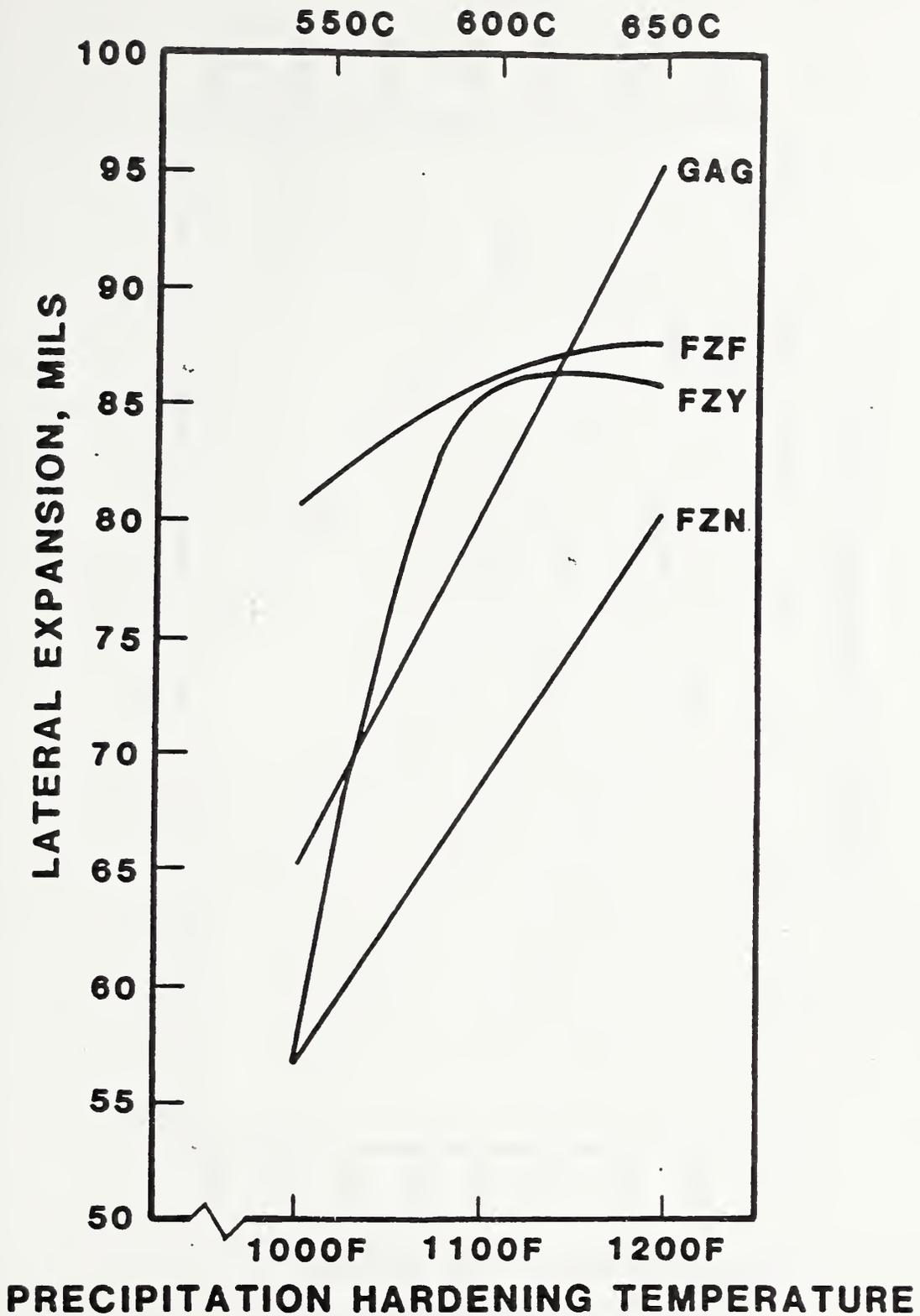
Figure 10   Lateral expansion of CVN impact specimens as a function of aging temperature. All samples aged for 30 minutes.

30
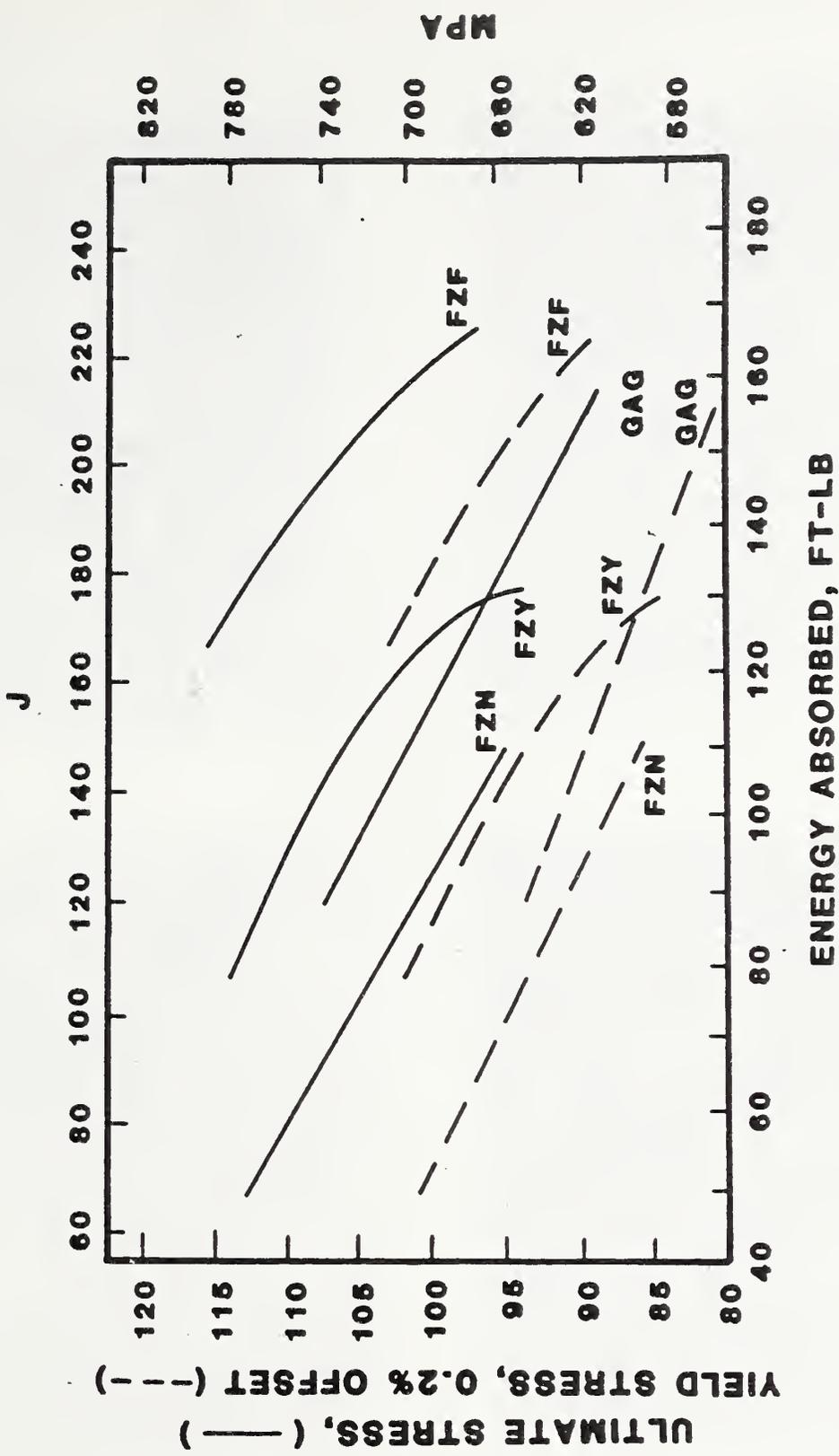
Figure 11 UTS and yield strength of the various plates versus energy absorbed in CVN impact tests.
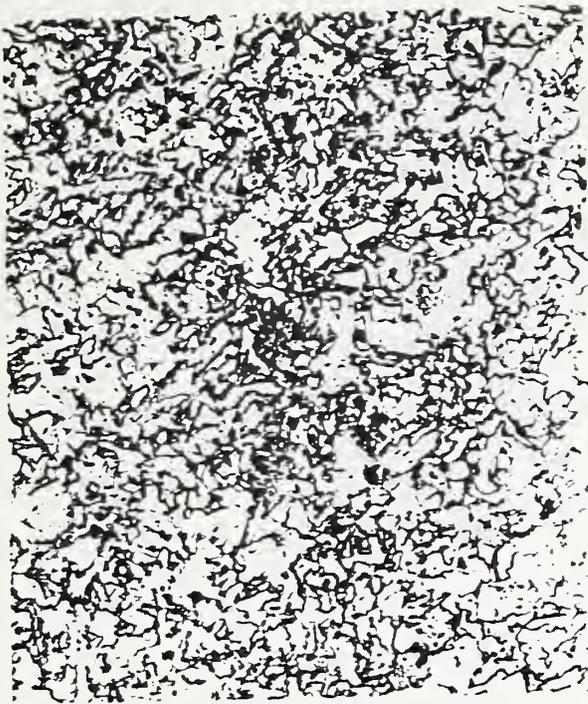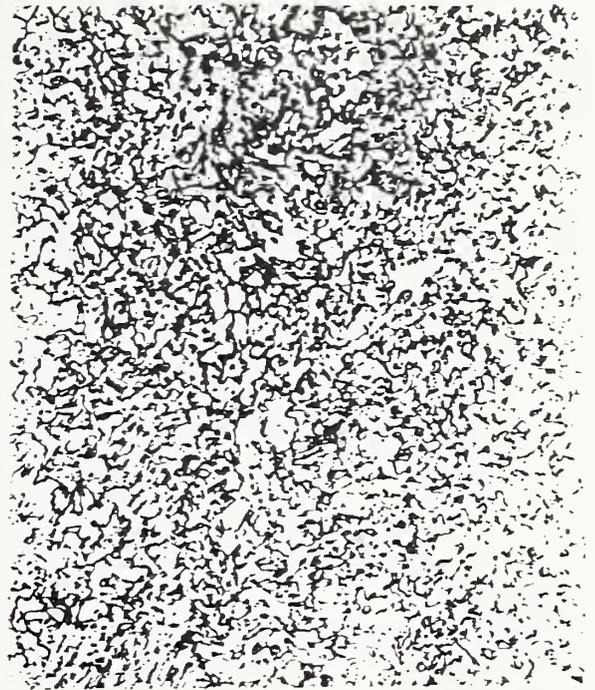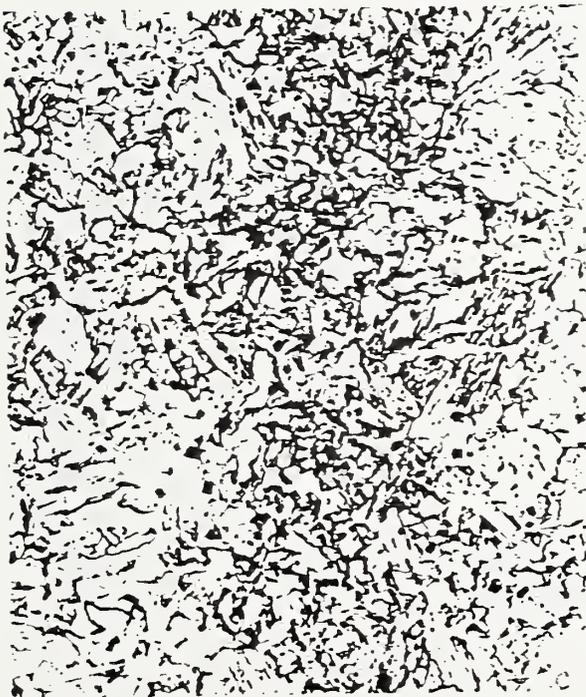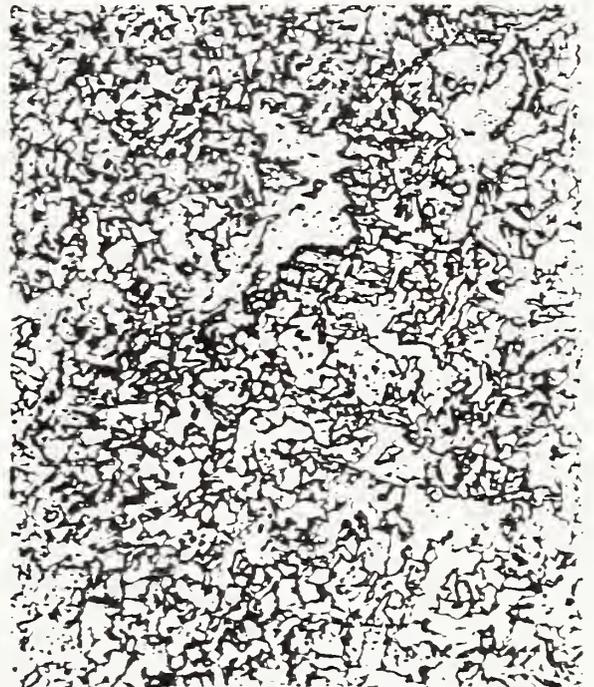
Figure 12   Optical micrographs at X500 (a) GAG, (b) FZF,
            (c) FZN, and (d) FZY. All 899°C (1650°F), 68
            min, WQ, 593°C (1100°F), 30 min, AC.
            Etchant: $(NH_4)_2MoO_4$ - HNO_3 in ethanol.
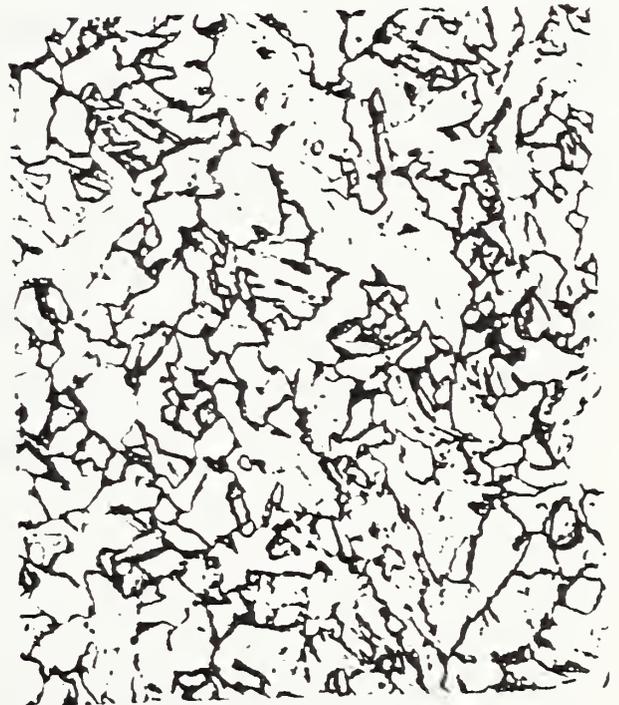
Figure 13 Optical micrographs at X1250 of heat treated
(a) GAG, (b) FZF, (c) FZN, and (d) FZY.
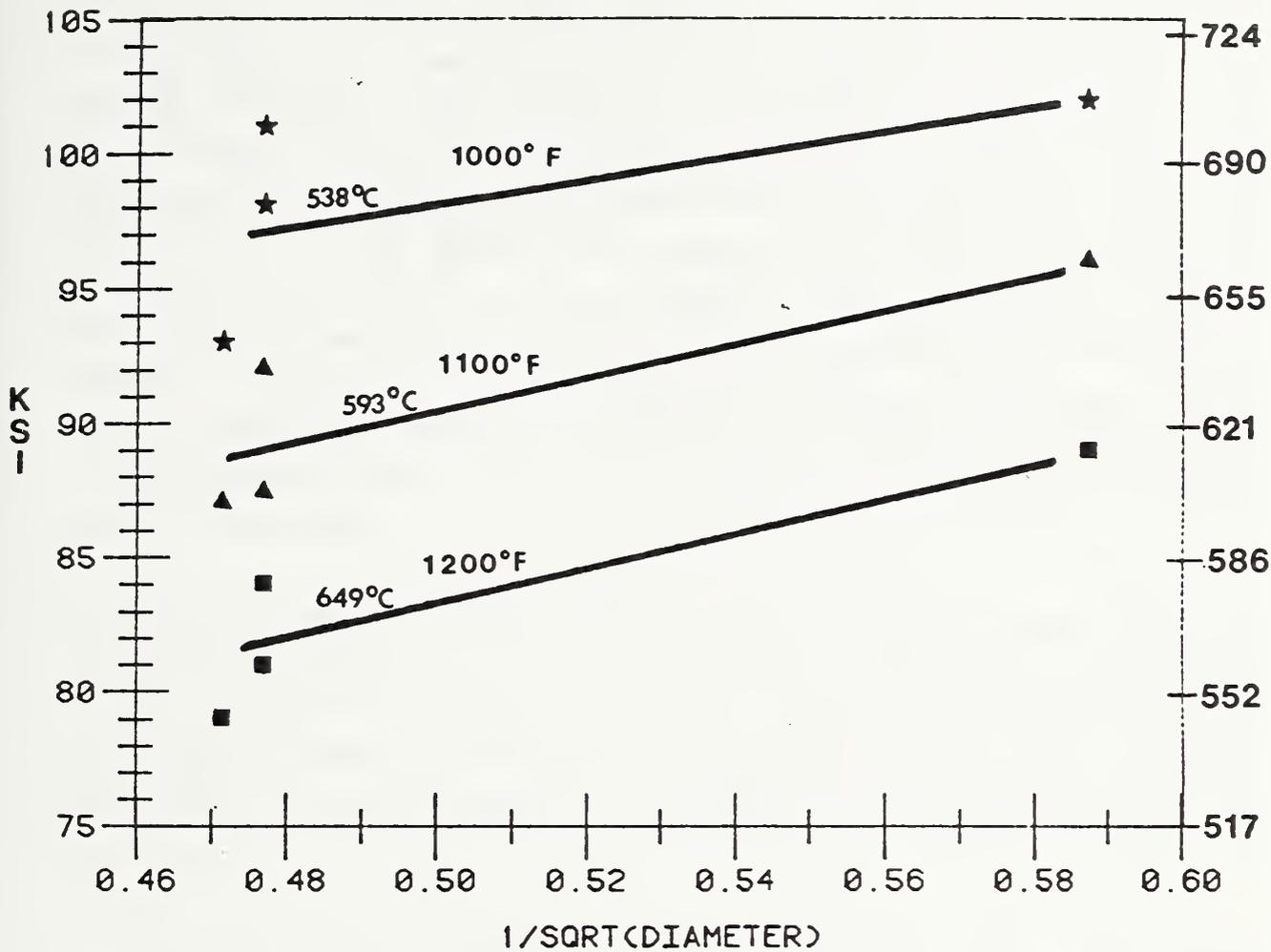
Figure 14   Hall-Petch plot: yield strength versus inverse
square root of grain diameter.

34

Appendix A - Longitudinal Splitting during Fracture

It was previously observed that fractured tensile bars of A710 occasionally exhibited deep(5-10 mm) longitudinal cracks or splits (Figure A1). These cracks formed slightly before or just at the moment of fracture. These cracks were distributed radially and were not associated with rolling anisotropy. Consultation with an expert in this field (A1) indicated that these cracks were an extreme form of star fracture [also called spoke-shaped fracture (A2) or "Fraserbruche" (milling cutter fracture) (A3)]. The origin of this name can be seen in a less severely split specimen (Figure A2). Radially distributed, shear escarpments are seen which resemble a star. Since the splitting is only observed in the necked portion of the specimen, its cause could be the high triaxial stress state or the high strain state that occurs there. If the splitting were caused by a triaxial (or constrained) stress state, use of A710 might be impeded. Service stresses are usually multiaxial, and reduction in ductility by such loading would be of concern. However, if a high plastic strain state were the cause of splitting, then no concern would be warranted as the ductility is virtually exhausted when splitting finally does occur and could be regarded as an artifact of a highly ductile fracture mode.

To investigate this phenomenon further, a plate of A710 was heat treated to the condition found to be prone to splitting in this investigation 899°C (1650°F), 30 min, WQ precipitation hardened - 538°C (1000°F) for 90 min and AC). Oversized tensile specimens [19 mm (3/4 inch) diameter gage sections] were machined from this plate. At fracture, these exhibited splitting (Figure A3).

Specimens were also fabricated which had a contoured notch. This notch matched the shape of the necked portion of the tensile specimens at the point of splitting (Figure A4). On loading, the stress state in this notched specimens would match that in the necked tensile bar at the point of splitting. If splitting was a stress state effect, then this notched specimen should exhibit splitting after very little plastic strain. In addition, several severely notched specimens were also fabricated (Figure A5). On

loading, these specimens would generate a very high triaxial (almost hydro-static) tension in the neck region. Any dependence of splitting on stress state should become obvious in these specimens.

The results of the tests are as follows:

Specimen	Max. tensile Stress		Fracture Appearance
	MPa	(ksi)	
Unnotched	780	(113)	Splitting
Contoured Notch	1014	(147)	No splitting
Severe Notch	1463	(212)	No splitting

Fractographs of the contoured notch and severely notched specimens are shown in Figure A6. Although exceedingly high stress elevations were obtained, these specimens did not exhibit any trace of splitting. In addition, the notched and severely notched specimens had reduced elongations to fracture.

The above results indicate that splitting is not caused solely by the triaxial stress state in the neck region. The fact that the unnotched specimen exhibited splitting and the contoured notch specimen did not suggests that a considerable plastic strain is required. It is likely that both the plastic strain and triaxial stress state are required to cause splitting. It is known that ductile cavities are formed around inclusions and large, second phase particles. The nucleation and growth of these cavities is determined by the plastic strain. The linkage and, in particular, the direction of linkage of these cavities to form the fracture surfaces is determined by the stress state.

Since considerable plastic strain is required to form ductile cavities, splitting cannot occur until well past the onset of necking. As engineering alloys are generally not expected to support strains of this magnitude (20-30%) in service, the occurrence of splitting seems to be inconsequencial. The reason why splitting occurs for some heat treated conditions and not others is unknown, although the above experiments suggest that the requirements for nucleation of ductile cavities has been somehow altered by the heat

36

treatments. Since the splitting does seem to be innocuous, however, the fundamental cause of splitting may be only of academic interest. Recent, unpublished, German research on this type of fracture also concludes that such splitting phenomena are innocuous (A4).

References

A1. J. Knott, Cambridge University, private communication.

A2. A.S. Tetelman and A.J. McEvily, Jr., Fracture of Structural Materials, p. 99, John Wiley and Sons, New York (1967).

A3. Riss-und Brucherscheinungen bei Metallischen Werkstoffen (The Appearance of Cracks and Fractures in Metallic Materials), Verlag Stahleisen mbH, Cusseldord (1983).

A4. A. Fuchs, German Society of Testing Materials (DVM), private communication.

a
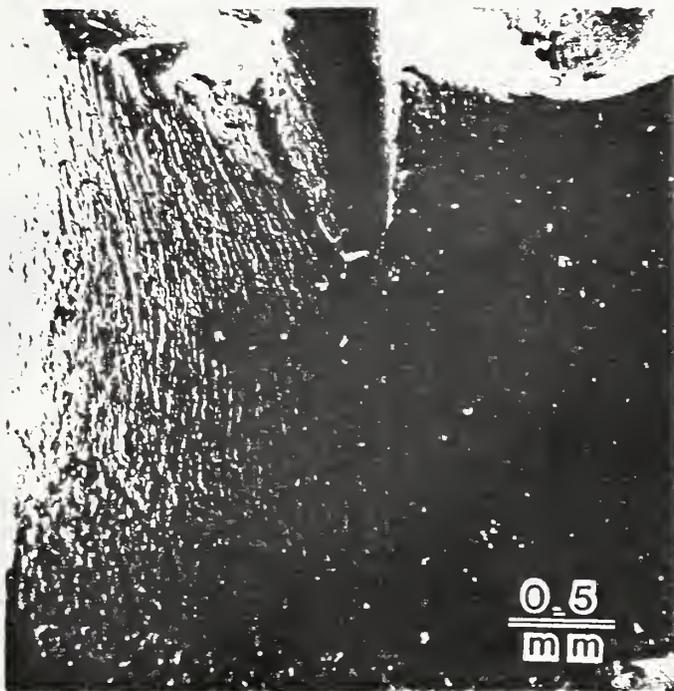
b

Fig. A1 Optical and SEM micrographs of splitting in A 710 tensile specimens.

38
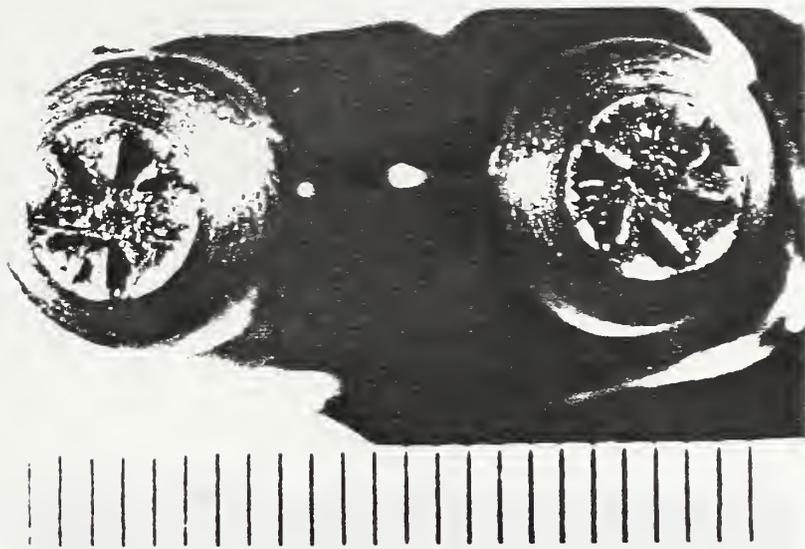
a
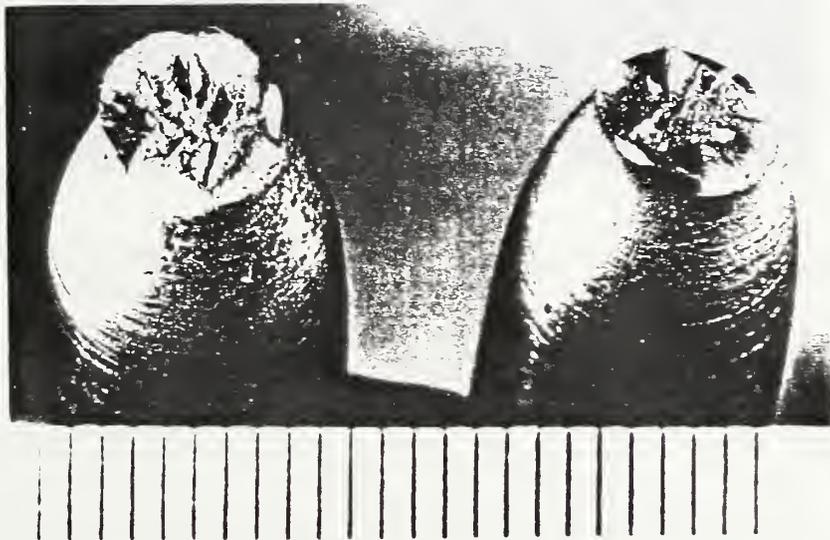
b

Fig. A2 Star fractures in A 710. Also known as spoke-type or milling
cutter fractures.

39
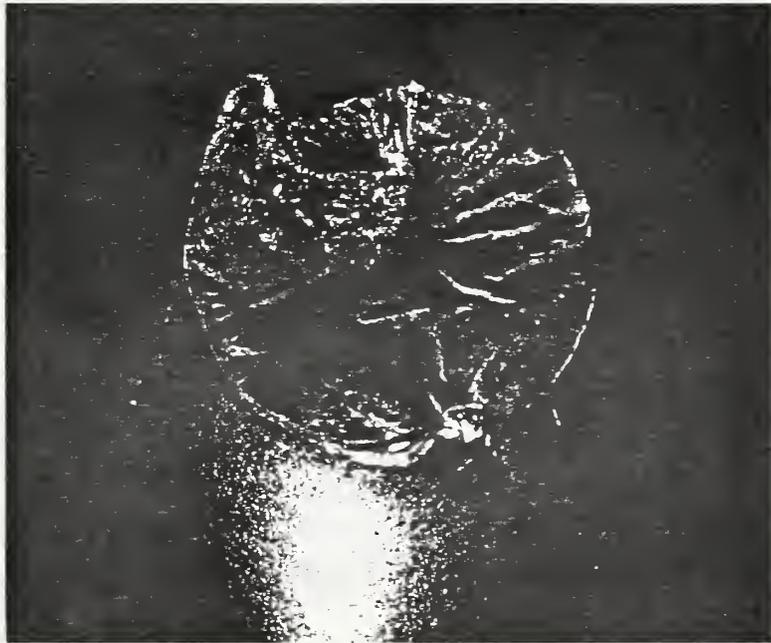
Fig. A3   Splitting observed in oversized (3/4" diameter gage) tensile
          specimen.
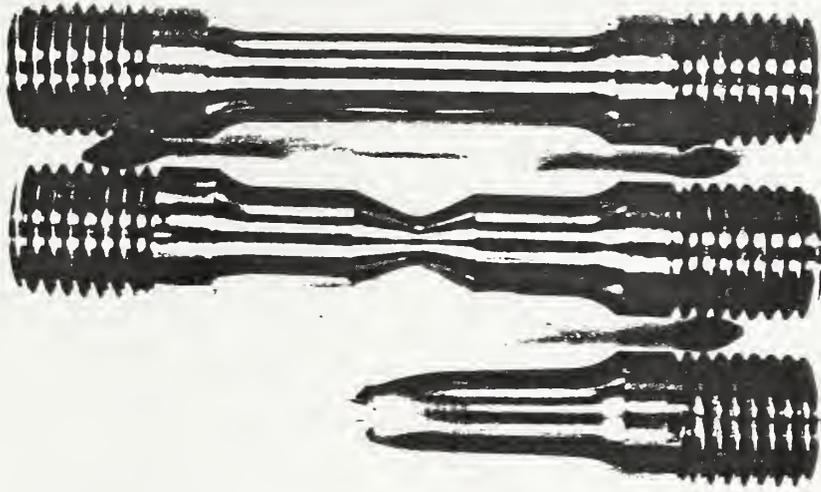
a

b

Fig. A4   Contoured notch specimen mimics curvature in neck of fractured
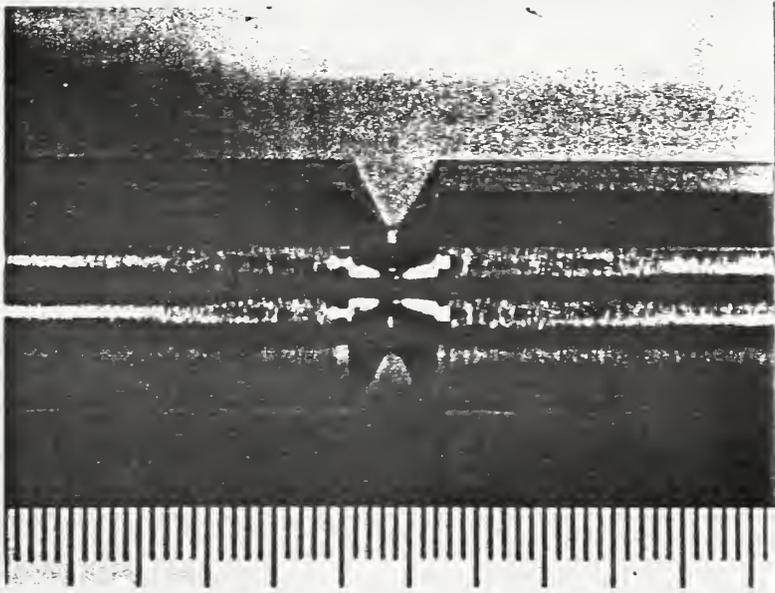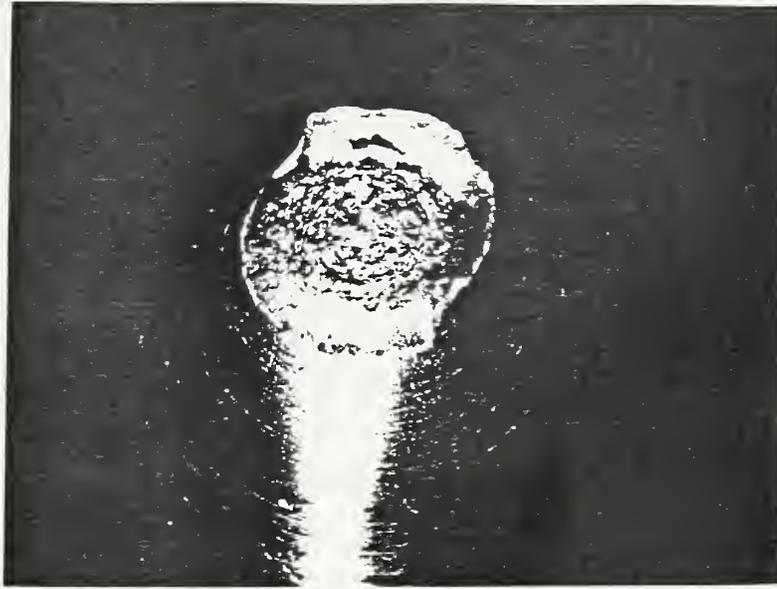tensile specimen which exhibited splitting.

Fig. A5   Severely notched specimen.

a

b

Fig. A6 Fracture surfaces of (a) contoured notch, and (b) severe notch. No evidence of splitting or even radial escarpments (star) is visible even though this is exactly the same heat-treated material as shown in Fig. A3.

43

Appendix B - Microchemical Observations

In the course of the TEM and SEM studies on A710, certain notable features were observed. One of the most frequently observed particles is shown in figure B1. This is a large (0.2 micrometer diameter) spherical particle. It is typical of particles which were found in all heats of A710. Sometimes it is more finely distributed. It was, at first, mistakenly identified as the ε-copper precipitate which is the main strengthening particle of A710. However, its large size and large interparticle spacing is too great to provide much strength. It was then thought to be the niobium carbo-nitride. This is also unreasonable as such a small amount of niobium is present and niobium usually occurs as an ultrafine dispersion. Using energy dispersive x-ray analysis in the TEM, two spectra were obtained (Figure B2a and b); the first being the matrix away from the particle, and the second is a spectra of a field containing the particle. From these two spectra, it can be seen that this particle is very rich in copper and sulphur. The presence of such a large particle could not have arisen by normal precipitaion of the copper. It is possible that these copper-rich particles are the result of incomplete mixing of the original metallurgical copper addition to the melt.

In the evaluation of the properties of another 3/4 inch thick A710, Class 3 plate supplied by DTNSRDC (Material Code GCM), erratic Charpy toughness values were found especially at low temperatures and for both orinetations. The chemistry and mechanical properties are shown in Table B1. During investigations by NBS of several impact specimens which had exhibited very different toughnesses, two other microstructural features were investigated. The first feature was a shiny phase which was unetched by nital (Figure B3). Energy dispersive x-ray spectra (Figure B4) indicated that these particles were rich in chromium. This again suggests that complete mixing of alloying additions had not taken place in the melt. The presence of this chromium rich phase was probably not the cause of the observed toughness variability. It was found in both the tough and the brittle Charpy specimens and was not associated with the fracture surface in either case.

On the other hand, a large (40-50 micrometer diameter) non-metallic inclusion was found on the fracture surface near the tip of the V-notch in the brittle specimen (Figure B5). Energy dispersive x-ray analysis (Figure B6) indicated

that this was an alumino-silicate slag inclusion. Without an inclusion
concentration analysis, it cannot be definitely concluded that an anomalously
high inclusion concentration is responsible for the high variability in
toughness. However, it certainly appears that there are visibly more slag
inclusions than usual in this particular plate (GCM) and such a situation
would result in highly varying toughnesses.

The observations of copper and nickel-chromium globules and large slag
inclusions may be indicative of irregularities in melting practice. Whether
or not such irregularities are of concern to the user of A710 can only be
determined by field experience. It is known, however, that large slag
inclusions are detrimental to properties and these should be tightly con-
trolled by appropriate steel making practice.

TABLE B1
Chemistry and Properties of 3/4 inch thick A 710, Class 3 Plate,
Material Code GCM

Producer Ladle Chemical Analysis (wt %)

C	Mn	P	Cr	Ni	Mo	Cu	Nb
0.05	0.69	0.010	0.83	0.92	0.19	1.20	0.040

Average Transverse Tensile Properties (DTNSRDC)

0.2% Yield Strength	Ultimate Tensile Strength	Elongation in 50 mm (2 in)	Reduction in Area
625 MPa (90.7 KSI)	708 MPa (102.7 KSI)	35%	76%

Charpy V-Notch Impact Toughness   (DTNSRDC)

| Test Temperature °C	(°F)	Impact Energy J (ft-lb) T-L Orientation	L-T Orientation
22.2	72	228 (168)	255 (188)
		236 (174)	248 (183)
		-	230 (170)
-17.8	0	218 (161)	225 (166)
		179 (132)	218 (161)
		-	197 (145)
-51	-60	159 (117)	180 (133)
		136 (100)	178 (131)
		-	56 (41)
-62	-80	131 (97)	183 (135)
		126 (93)	167 (123)
		41 (30)	161 (119)
-73	-100	89 (66)	87 (64)
		81 (60)	37 (25)
		26 (19)	31 (23)
-84	-120	57 (42)	80 (59)
		76 (56)	46 (34)
		-	24 (18)

Fig. B1 Transmission electron micrograph of frequently
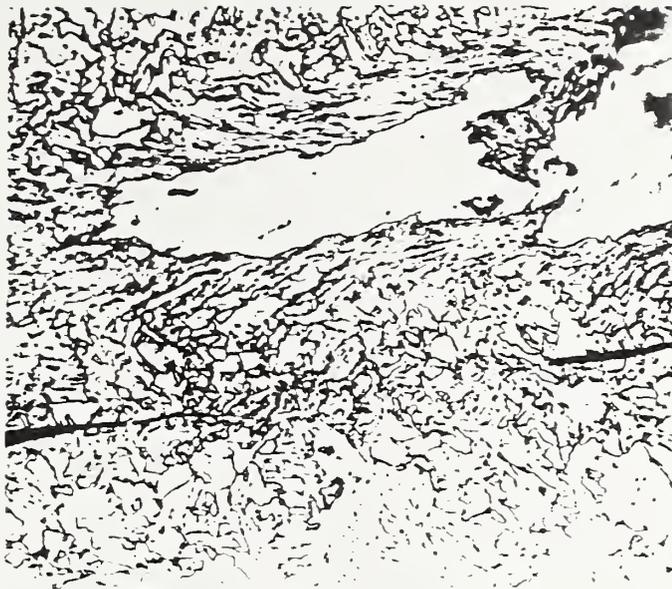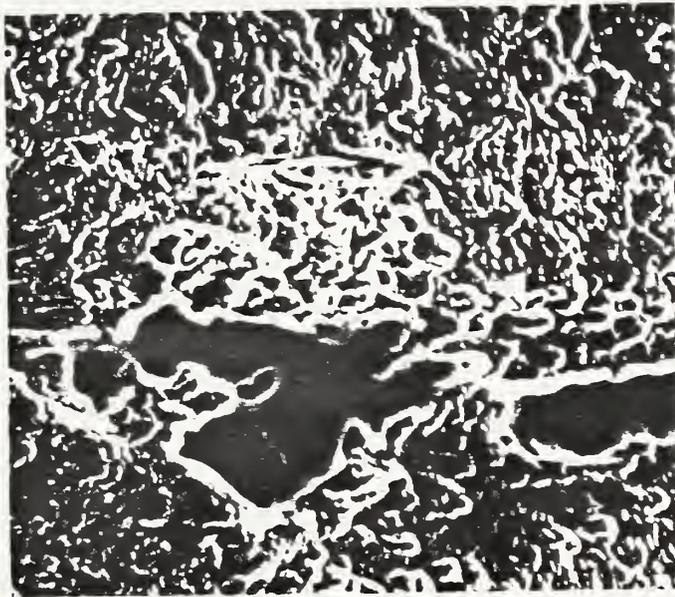observed, large particle in A 710. X60,000
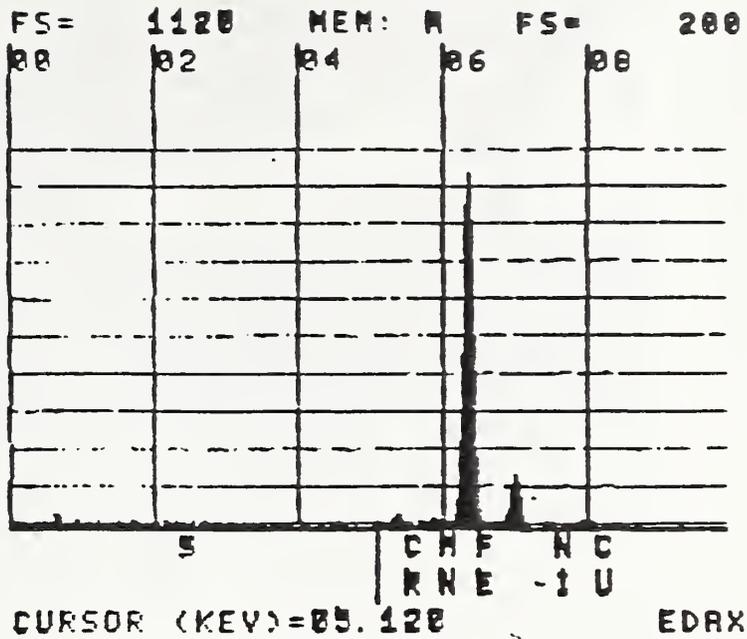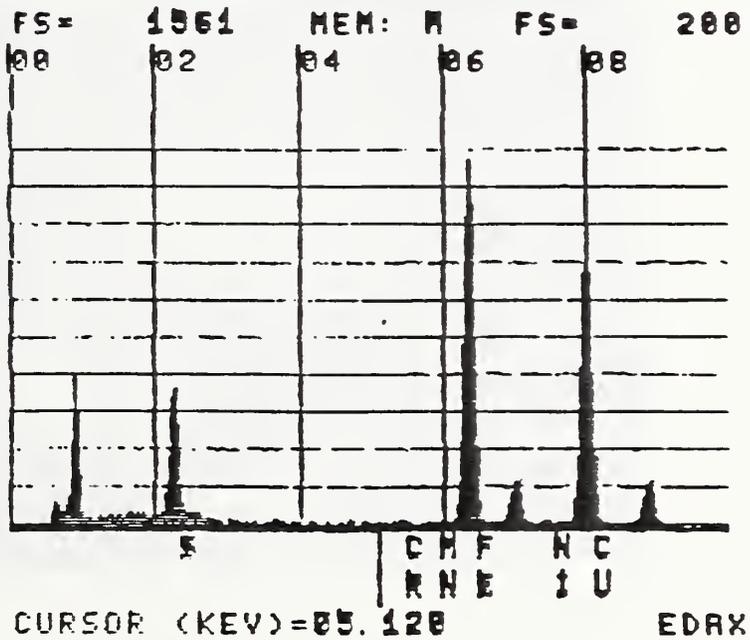
Fig. B2 Energy dispersive x-ray spectra of (a) matrix, and (b) matrix plus particle. Note high copper and sulphur intensities.
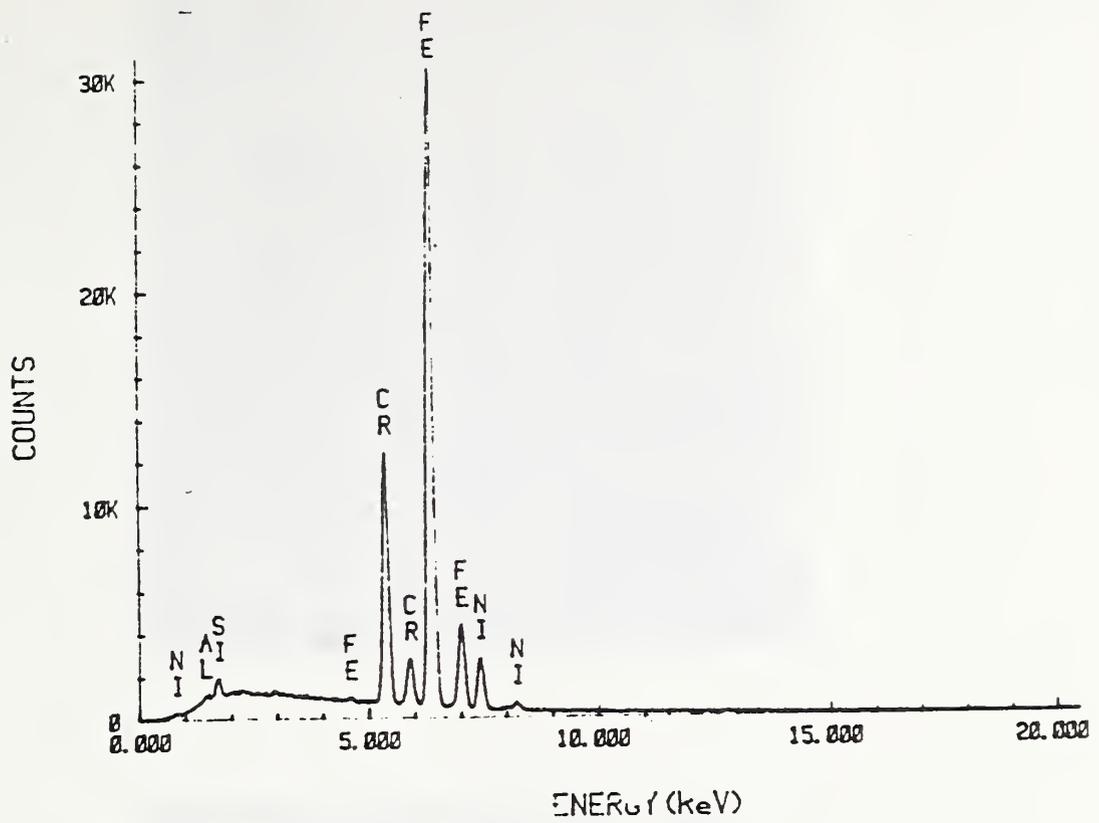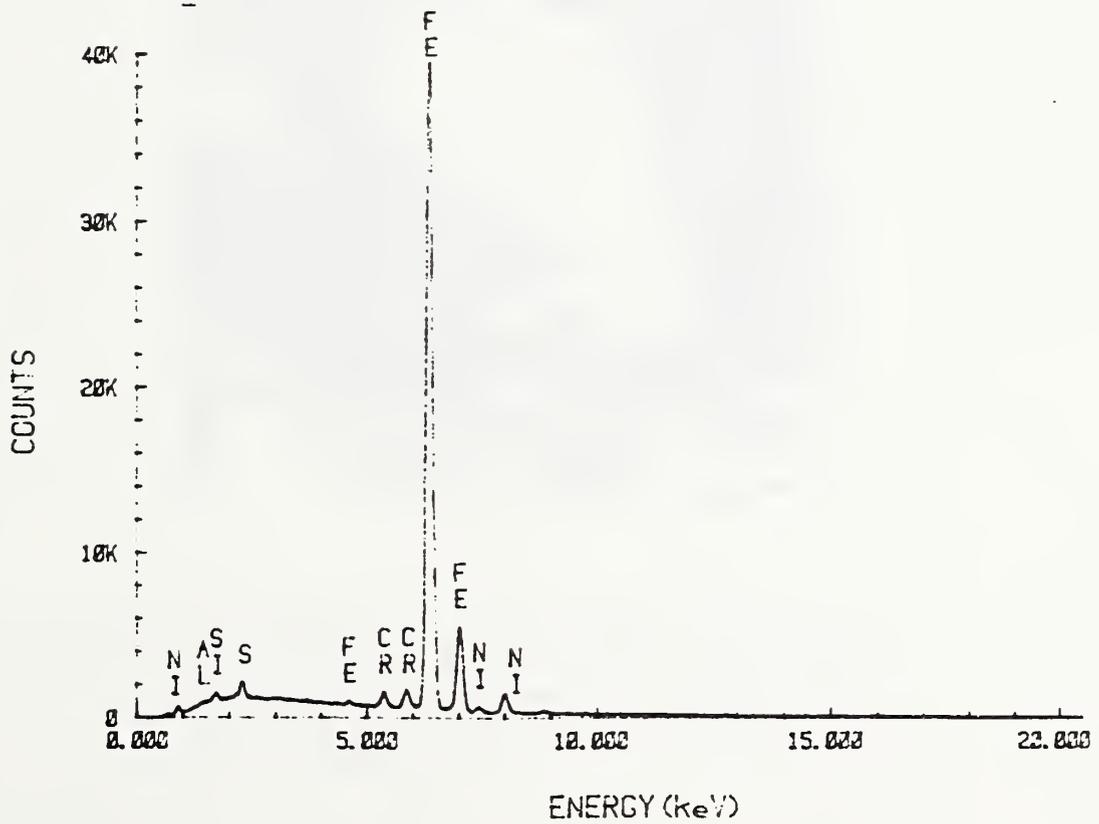
a

b

Fig. B3 Unetchable, shiny particles that were found in plate
having variable impact properties. (a) X500,
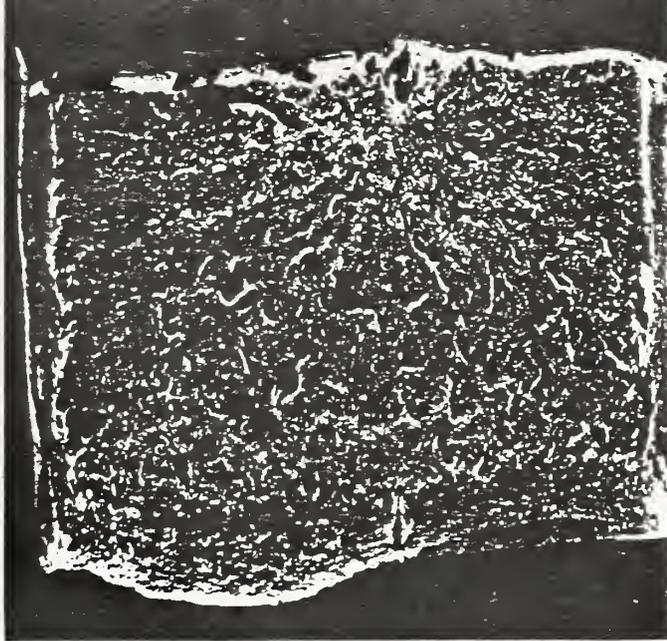(b) X742. Etchant: 1% Nital.
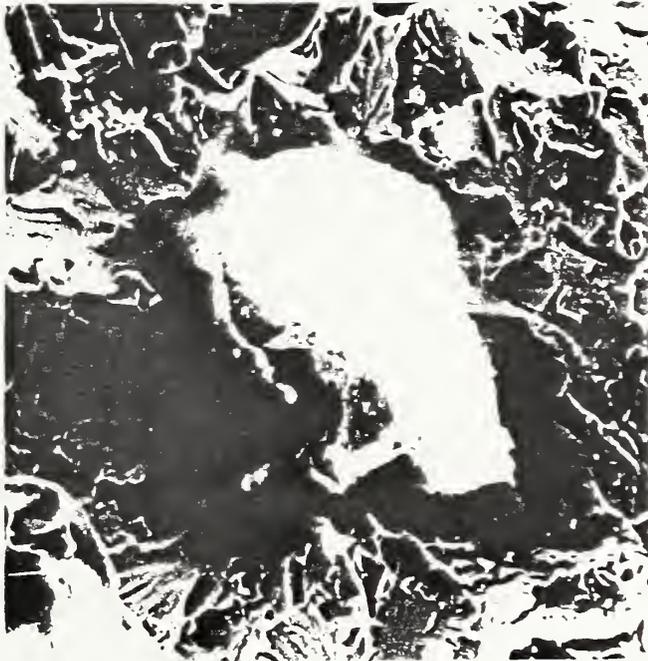
Fig. B4 Energy dispersive x-ray spectra of (a) shiny particle
plus matrix, and 9b) matrix. Note high chormium peak
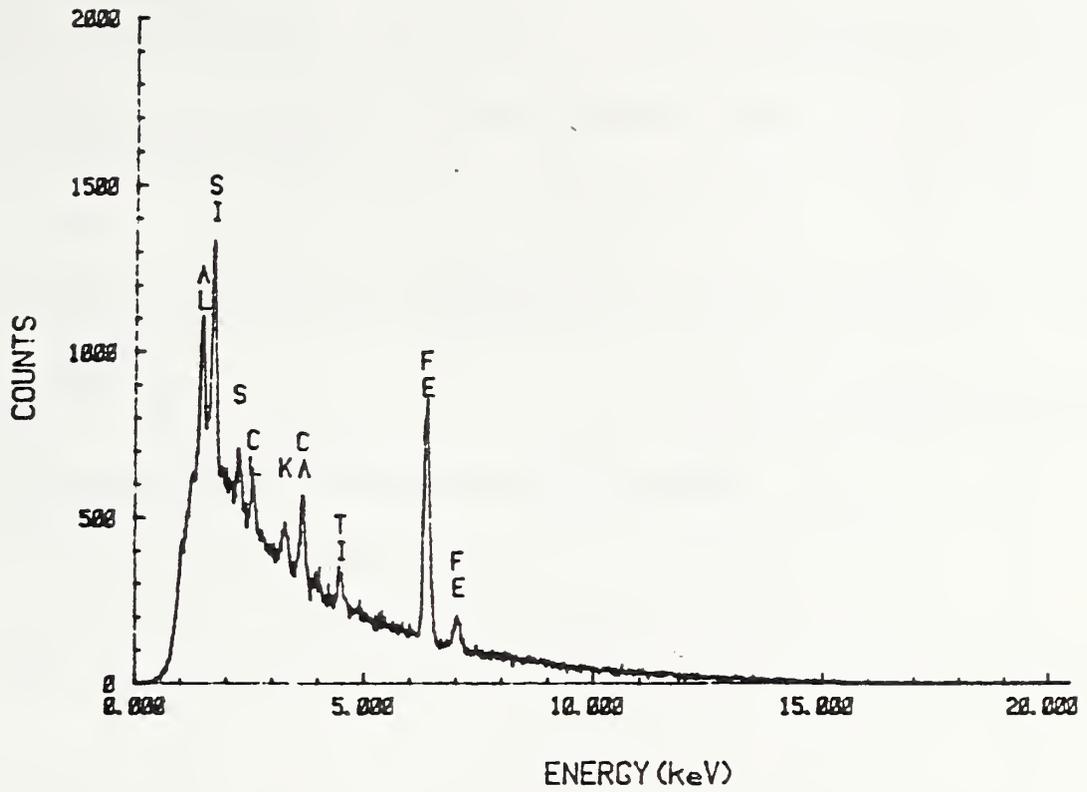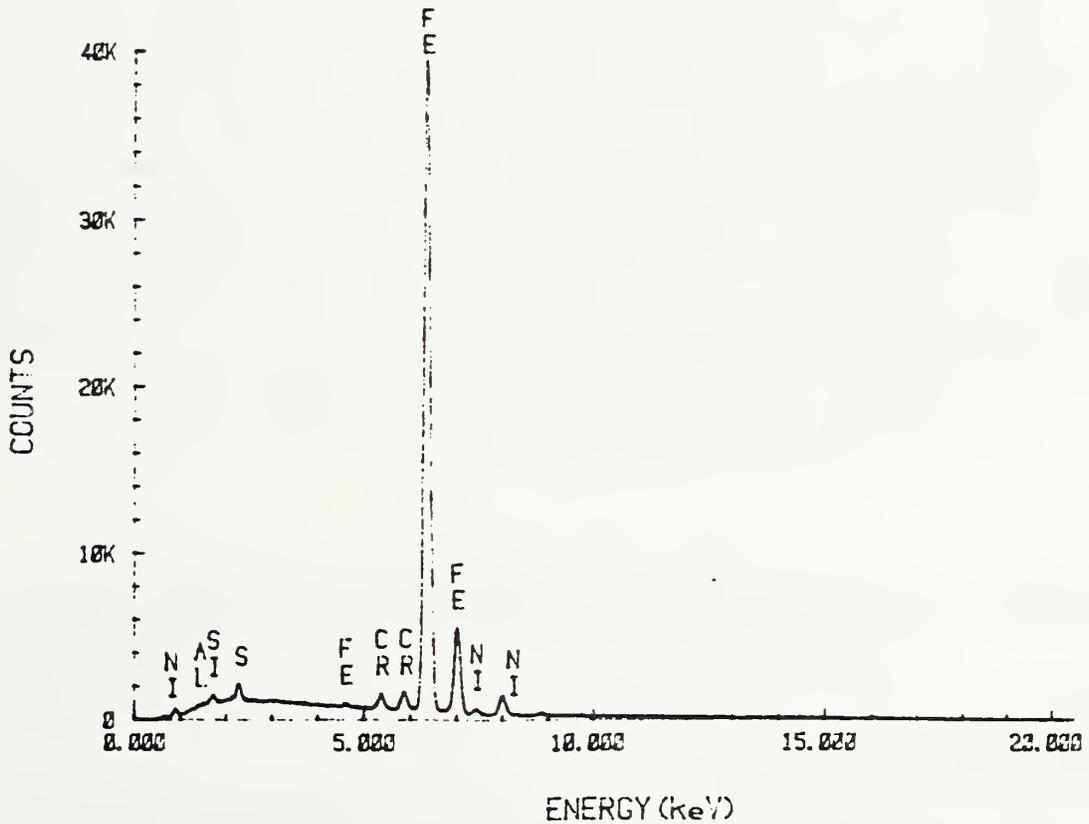coming from particle.

50

a

b

Fig. B5 (a) Fracture surface of impact specimen having
anomolously low toughness, X7. (b) High
magnification (X684) near the notch root shows
large inclusion (40-50 μm dia.) responsible for
low toughness value.

51

Fig. B6   Energy dispersive x-ray spectra of (a) inclusion plus
           matrix, and (b) matrix alone. Note high silicon and
           aluminum peaks coming from inclusion.

BS-114A (REV. 2-8C)

U.S. DEPT. OF COMM. **BIBLIOGRAPHIC DATA SHEET** (See instructions)	1. PUBLICATION OR REPORT NO. NBSIR 84-2891	2. Performing Organ. Report No.	3. Publication Date MARCH 1985

4. TITLE AND SUBTITLE

"Effect of Heat Treatment on Mechanical Properties and Microstructure of Four Different Heats of ASTM A710 Steel"

5. AUTHOR(S)

G.E. Hicho, C.H. Brady, L.C. Smith, R.J. Fields

6. PERFORMING ORGANIZATION (If joint or other than NBS, see instructions)

NATIONAL BUREAU OF STANDARDS
DEPARTMENT OF COMMERCE
WASHINGTON, D.C. 20234

7. Contract/Grant No.

8. Type of Report & Period Covered

10. SUPPLEMENTARY NOTES

☐ Document describes a computer program; SF-185, FIPS Software Summary, is attached.

11. ABSTRACT (A 200-word or less factual summary of most significant information. If document includes a significant bibliography or literature survey, mention it here)

A710 is an HSLA steel whose strength is a result of both a fine grained microstructure and a dispersion of copper precipitates. For these reasons, the tensile and impact properties of an A710 plate depend as much on the thermo-mechanical history of each plate as on the chemistry of each heat. Since plates shipped from steel suppliers are frequently heat treated under different conditions, it is difficult to attribute property differences to chemistry variations rather than to heat treatment variations or vice versa. Heat to heat property differences must be determined for a specific, known heat treatment. This report describes the variability in the mechanical properties of four plates (representing four heats of steel) that have received known, and carefully controlled, heat treatments at the National Bureau of Standards. The sensitivity of these properties to heat treatment variations within each heat of steel is also reported here. Optical and electron metallographic techniques were used to determine as-received and heat treated microstructures. Scanning electron fractography was used to ascertain the fracture mechanism in the tensile and impact tests. This report also contains two appendices in which splitting fracture and microchemistry observations in A710 are discussed.

12. KEY WORDS (Six to twelve entries; alphabetical order; capitalize only proper names; and separate key words by semicolons)

A710 HSLA steel; grain size; fractography; heat treatment; impact properties; microstructure; tensile properties.

13. AVAILABILITY	14. NO. OF PRINTED PAGES
☒ Unlimited	
☐ For Official Distribution. Do Not Release to NTIS	43
☐ Order From Superintendent of Documents, U.S. Government Printing Office, Washington, D.C. 20402.	15. Price
☒ Order From National Technical Information Service (NTIS), Springfield, VA. 22161	$8.50